Cell Host & Microbe, Volume *17*

Supplemental Information

Stressed Mycobacteria Use the Chaperone ClpB to Sequester Irreversibly Oxidized Proteins Asymmetrically within and between Cells

Julien Vaubourgeix, Gang Lin, Neeraj Dhar, Nicolas Chenouard, Xiuju Jiang, Helene Botella, Tania Lupoli, Olivia Mariani, Guangli Yang, Ouathek Ouerfelli, Michael Unser, Dirk Schnappinger, John McKinney, and Carl Nathan

Supplemental Information for:

Asymmetric distribution of irreversibly oxidized, ClpB-associated proteins in stressed mycobacteria

Julien Vaubourgeix[1], Gang Lin[1], Neeraj Dhar[2], Nicolas Chenouard[4], Xiuju Jiang[1], Helene Botella[1], Tania Lupoli[1], Olivia Mariani[3], Guangli Yang[5], Ouathek Ouerfelli[5], Michael Unser[3], Dirk Schnappinger[1], John McKinney[2], and Carl Nathan[1]*.

Supplemental Figure Legends

Figure S1. **IOP accumulate in mycobacteria,** related to Figure 1.

(A) Detection of increasing amounts (ng) of DNPH-treated BSA or DNPH-treated oxidized BSA (oxBSA) with anti-DNP antibodies. Oxidized BSA was prepared as described (Maisonneuve et al., 2009).

(B) Detection of DNPH-treated BSA or DNPH-treated oxidized BSA (oxBSA) by colorimetry (371 nm). Un-treated BSA, oxBSA, and the buffer used for solubilizing treated samples served as controls. N = 3 experiments.

(C) Accumulation of IOP in *Msm* in stationary phase (STAT) compared to logarithmic phase (LOG). N = 2 replicates of one experiment.

(D) Protein carbonyl content of BCG in logarithmic phase (LOG), when subjected to 5 mM H_2O_2, and in stationary phase (STAT). The carbonyl content was assessed in the soluble fraction (S) or both in the soluble (S) and the insoluble (I) fractions (S+I). N = 3 experiments.

(E) Identities of carbonylated proteins covalently captured using beads bearing a hydrazide from Mtb's protein lysates recovered with buffer supplemented with 5% SDS. Given that carbonylation can confound identification of peptides, the 67 proteins were scored for study by

an algorithm that includes the Mascott hit score ($S_{Mascott}$); number of peptides used for identification (N_{pep}); ion count of each peptide ($\bar{O}_{pep}$); molecular weight of the protein (MW); concordant identification performing the same experiment with *M. bovis* BCG (P_{BCG}); and prediction of propensity for carbonylation (termed hot spot for carbonylation, HSC) by the algorithm of Maisonneuve et al. (P_{HSC}) (Maisonneuve et al., 2009). Homologs of IOP in other bacteria identified as IOP in stationary phase or following aminoglycoside-induced mistranslation or hydrogen peroxide exposure are marked in bold: glutamine synthetase A1 (Rv2220), histone-like proteins (Rv2986c), elongation factor EF-Tu (Rv0685), NADP-dependent alcohol dehydrogenase AdhC (Rv3045) and the 60kDa chaperonin GroEL (Rv0440) (Dukan et al., 2000; Dukan and Nyström, 1999; Tamarit et al., 1998).

(F) Ability of the Atc-inducible Δ*MDP1*::pGMCS P1T10M *hupB-dendra2* complemented strain to grow similarly as wild-type *M. smegmatis* on plates containing 8 μg/mL of isoniazid (INH) when supplemented with sufficient concentrations of ATc, that is, near the Atc-impregnated disk in the center. In contrast, the MDP1 deletion mutant failed to form a lawn; instead, discrete colonies slowly appeared on the plates.

(G) Table summarizing the growth phenotypes captured in (A) of wild-type *M. smegmatis,* Δ*MDP1* and Δ*MDP1*::pGMCS P1T10M *hupB-dendra2* on 7H11 plates without INH or containing 8 μg/mL of INH.

Figure S2. **Construction of Δ*clpB* and Δ*MSMEG_0732* (ClpBSm)**, related to Figures 2 to 7.

(A) Organization of the genomic region encompassing *clpB* in Mtb H37Rv (top) and Δ*clpB* (bottom). Recognition sites of the restriction endonuclease PvuI are marked. The genomic fragment to which the probe used for Southern blotting (C) binds is designated by a line (Probe). Plasmids encoding ClpB-GFP or ClpB-Dendra2 were expressed in Δ*clpB* and Δ*MSMEG_0732* (B). The blue rectangle indicates a serine-glycine encoding repeat (x3). RS stands for

recombination site.

(B) Organization of the genomic region encompassing *MSMEG_0732* in Msm (top) and Δ*MSMEG_0732* (bottom). Recognition sites of the restriction endonuclease SacI are marked. The genomic fragment to which the probe used for Southern blotting (C) binds is designated as in (A).

(C) Southern blotting of PvuI-digested genomic DNA from H37Rv, H37RvΔ*clpB::clpB* (attL5, merodiploid strain), H37RvΔ*clpB::clpB* (Tweety, complementation strain) and Δ*clpB* (left) and SacI-digested genomic DNA from Msm and Δ*MSMEG_0732* (right).

(D) Western blots on protein lysates of *H37Rv* Mtb, H37Rv:Δ*clpB*, and H37Rv:Δ*clpB::ClpB* (top) and Msm, Δ*MSMEG_0732,* Δ*MSMEG*_0732::*MSMEG*_0732, Δ*MSMEG*_0732::ClpB (bottom) using ClpB antibodies (Mtb strains) or ClpB antiserum (Msm strains). 50 μg of total proteins were loaded per lane. ClpB in Msm (MSMEG_0732) and Mtb (ClpB) share 90.3% amino acid identity. Their expected masses are ~ 92.9 kDa and ~ 92.5 kDa, respectively.

Figure S3. **Engineering fluorescent ClpBs that are functional**, related to Figures 3 to 6.

(A) Ability of wild type *M. smegmatis*, Δ*clpB*, Δ*clpB*::*clpBsm*, Δ*clpB*::*clpB-gfp* and Δ*clpB*::*clpB-dendra2* to recover from prolonged stationary phase. While Δ*clpB* had a delayed recovery, the two ClpB-tagged versions each allowed recovery at a rate similar to wild type.

(B) Distribution of ClpB-GFP (green and carbonyls reactive with TR-APTAH (red) in MSm in logarithmic phase (LOG) and in stationary phase (STAT).

(C) Amino acid sequence of Dendra2. Chromophore-forming residues are colored in green; mutations in the original Dendra have been introduced respectively to disrupt tetramer interface (blue), to improve folding and chromophore maturation (orange) and to increase brightness (purple) (Gurskaya et al., 2006).

(D) Nucleotide sequence coding for Dendra2. Codons are those preferred by mycobacteria.

(E) Photoconversion of Dendra2 green signal into red after exposure to 405-nm light at illuminations low enough to avoid phototoxicity. The cross indicates where the 405-nm laser was directed. BPC, before photoconversion; APC, after photoconversion.

(F) Snapshots in the red channel were taken every 200 ms after photoconversion. The intensity of the red is displayed using false colors. Square and circle in panel for 0.7 s indicate regions at proximity and increased distance from the laser directed point (cross) that were used for quantification of photoconverted signal (red) in (E).

(G) Quantification of (D).

(H) Photoconversion of ClpB-Dendra2 green signal into red. BPC, before photoconversion; APC, after photoconversion. The cross indicates where the 405 nm laser was directed.

Figure S4. **Computational tools for the quantification of sequential images of mycobacteria and controlled expression of fluorescent versions of ClpB or PrcBA in Msm cells**, related to Figures 4 and 6.

(A) Continuous modulation of the threshold (blue) using SpotDetectorT, a customized SpotDetector plugin hosted by the open source software Icy (de Chaumont et al., 2012; Olivo-Marin, 2002). This algorithm compensates for time-dependent loss of fluorescence caused by photo-bleaching during sequential observations (pink). Photobleaching was scaled to a mono-exponential with > 95% mean accuracy, σ = 0.8. μ_k = 0.269, σ = 0.027; $\mu_{amplitude}$ = 36.1, σ = 2.5. Scripts are available on the Icy webpage (plugins section).

(B) Description of Mycomask or Mycoclump. This plugin converts the transmitted-light image (left) into a binary image (*Ib*, middle) (see methods). 4 values are attributed to each pixel (cross)—x, y, z (spatial coordinates) and 0 (background pixel) or 1 (bacterial pixel). The fluorescence intensity of unique bacterial pixel (Ip) identified in the binary image can be extracted from the fluorescent channel (right).

(C) Non-exhaustive list of mathematical parameters accessed using Mycomask or Mycoclump.

(D) GFP, ClpB-GFP and ClpBY251A-GFP are expressed in presence of anhydrotetracycline (Atc) (lanes 2, 4 and 6). Lanes 1, 3 and 5 correspond to no induction controls. GFP and the two GFP-tagged ClpB's were immunoblotted with anti-GFP antibody.

(E) PrcA-mCherry is expressed in presence of anhydrotetracycline (Atc) (lane 2). Lane 1, control with Msm transformed with mCherry alone (arrow). Lane 3, control with Msm transformed with PrcA-mCherry but not induced. mCherry and mCherry-tagged PrcA were immunoblotted with anti-mCherry antibody.

Figure S5. **ClpB-deficient Mtb is not hypersensitive to aminoglycosides or INH, but recovers more slowly than wild type**, related to Figure 7.

(A) Sensitivity of H37Rv, Δ*clpB* and Δ*clpB::clpB* to antibiotics. Minimum inhibitory concentration (MIC) of various drugs against wt and Δ*clpB*. MIC_{90} values in μg/mL, determined by minimum concentration at which OD_{600} was less than 10% that of untreated control.

(B) Defective recovery of ClpB-deficient Mtb from a 10-day exposure to sub-inhibitory concentrations of kanamycin (1.2 μg/mL) or streptomycin (0.3 μg/mL). The y-axis represents the number of generations from the onset of the outgrowth to days 5 (D5), 7 (D7) and 10 (D10). Mean ± SD of replicates in one experiment.

Figure S6. **Proposed models for the disposal of IOP,** related to Figures 5 and 6, and discussion.

(A) IOP (green) are diluted by cell division (Diffuse model, left).

(B) IOP (green) are asymmetrically distributed between descendants (Aggregation-Sequestration models, right). The stresses that generate IOP are likely to preclude cell division, so this remedy exposes the cell to the full content of IOP until division resumes, and to half as much in both members of the next generation. Cells could surround IOP with chaperones. Cells

could minimize the expenditure of chaperones in this dead-end activity by collecting IOP into the smallest possible number of aggregates, given that a single sphere affords the minimum surface area for a given volume. Cells could move the aggregated IOP to one location and shed them by pinching off a portion of the cell (Exclusion model, left panel; D1' indicates the fragment released by blebbing). This requires machinery for segmentation similar to that required for cell division, but unlinked from chromosomal replication. Finally, cells could aggregate IOP and distribute the aggregates asymmetrically between progeny (Selective retention, right panel).

Table S1. **Table of strains used in this study**, related to experimental procedures**.**

Table S2. **List of primers used in this study to introduce genetic alterations**, related to experimental procedures**.**

Movie S1. **Representative time-lapse microscopy image sequence of Δ*clpB*sm::*clpB-dendra2* subjected to a rest-stress-rest-stress-rest perfusion paradigm.** The stress applied was 1 μg/mL of kanamycin, related to Figures 3, 4, and 5.

Movie S2. **Representative time-lapse microscopy image sequence of *M. smegmatis* expressing ClpBY251A-GFP challenged with kanamycin,** related to Figure 4**.**

Movie S3. **Representative time-lapse microscopy image sequence of *M. smegmatis* expressing ClpB-GFP challenged with kanamycin,** related to Figure 4.

Movie S4. **Representative time-lapse microscopy image sequence of *M. smegmatis* expressing PrcBA-mCherry challenged with kanamycin,** related to Figure 4.

Movie S5. **Representative time-lapse microscopy image sequence of M. smegmatis expressing GFP challenged with kanamycin,** related to Figure 4.

Movie S6. **Representative time-lapse microscopy image sequence of Δ*clpB*sm::*clpB-dendra2* subjected to a rest-stress-rest-stress perfusion paradigm.** The stress applied was 40 μg/mL of INH**,** related to Figure 6.

Figure S1.

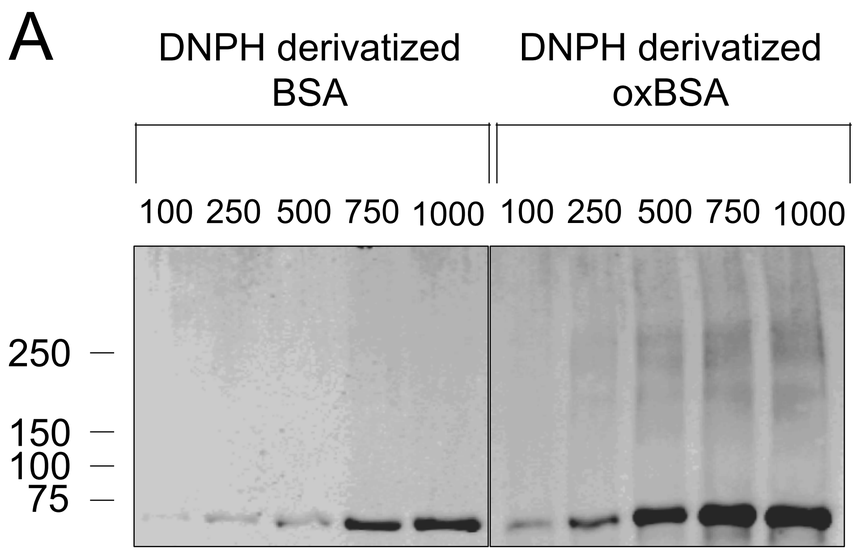

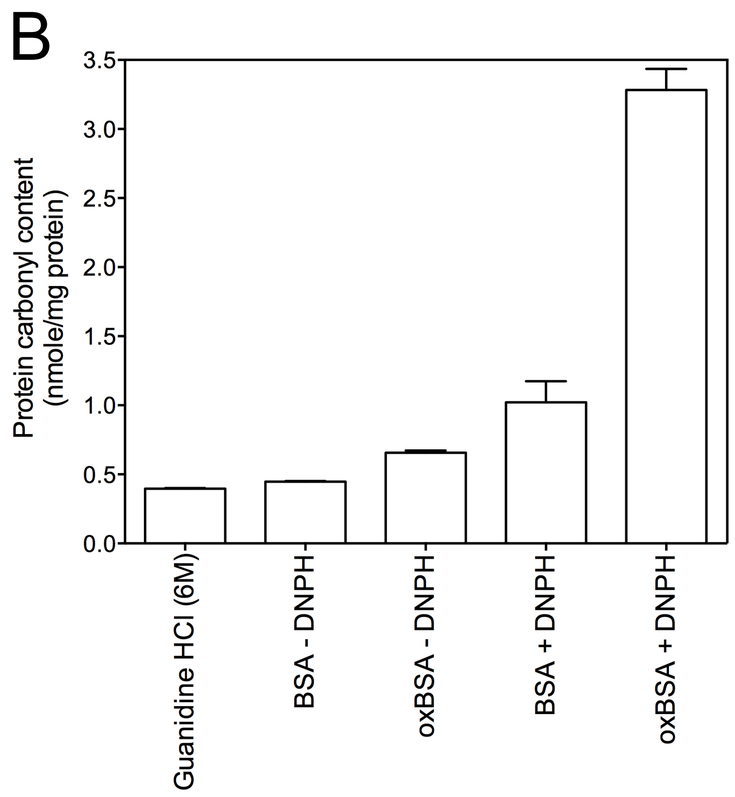

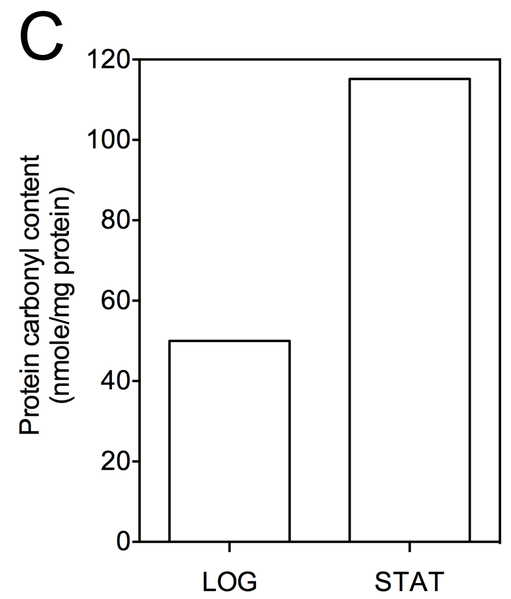

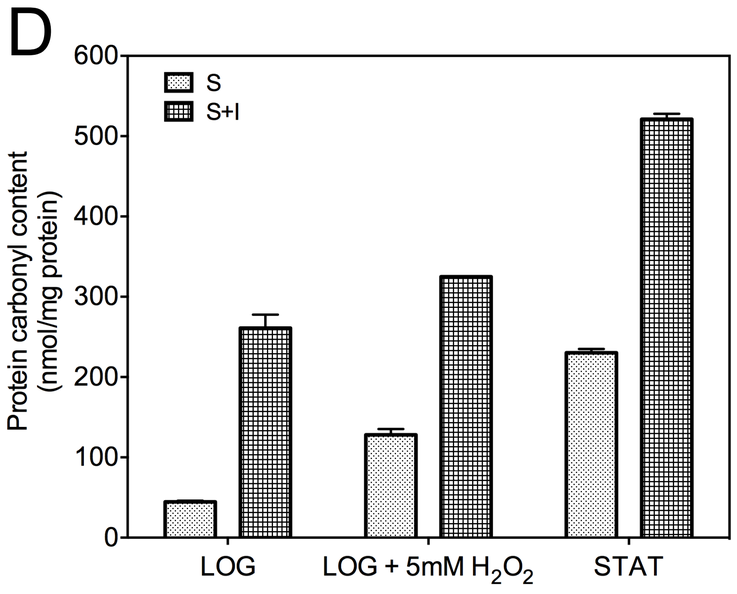

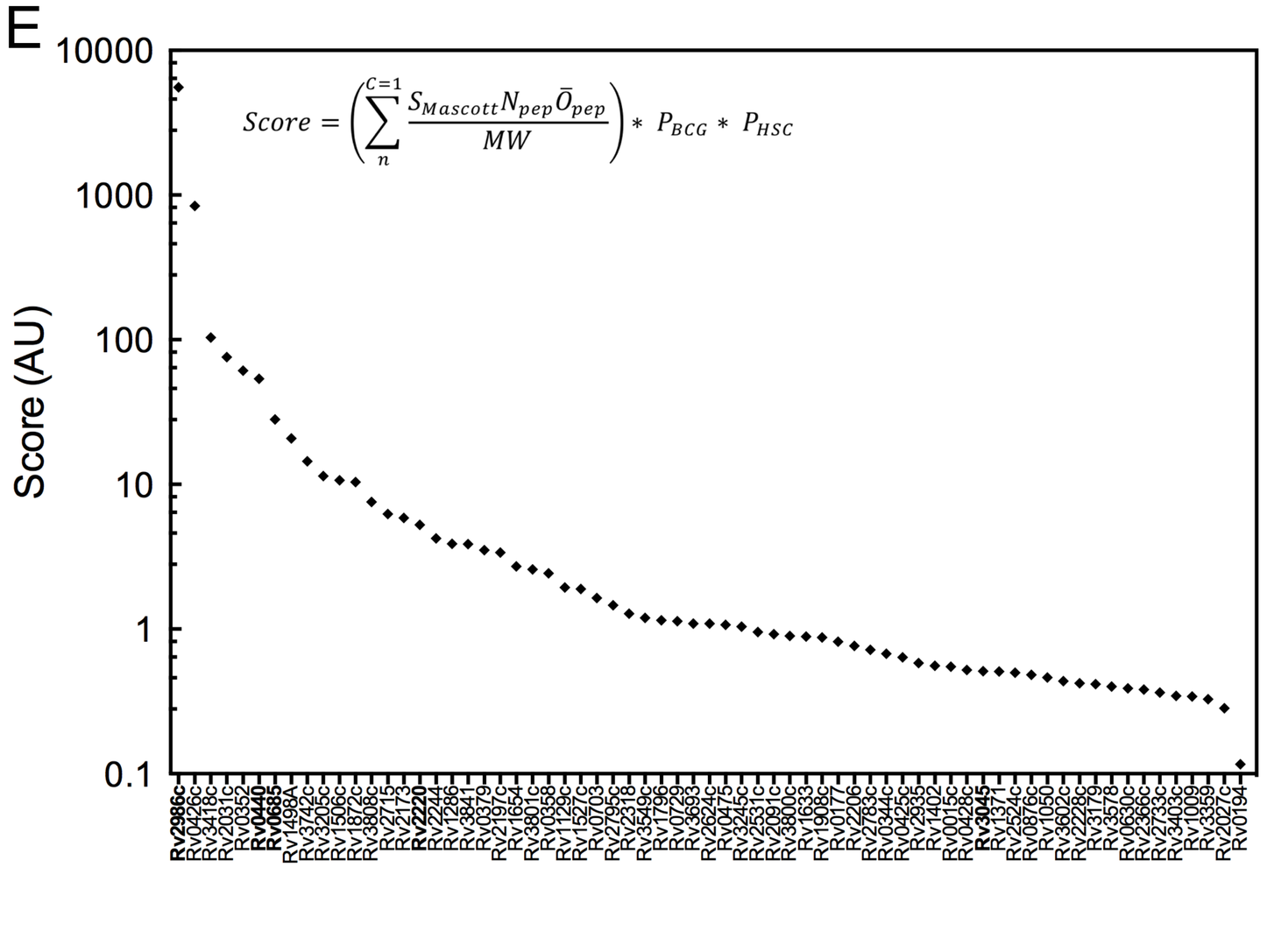

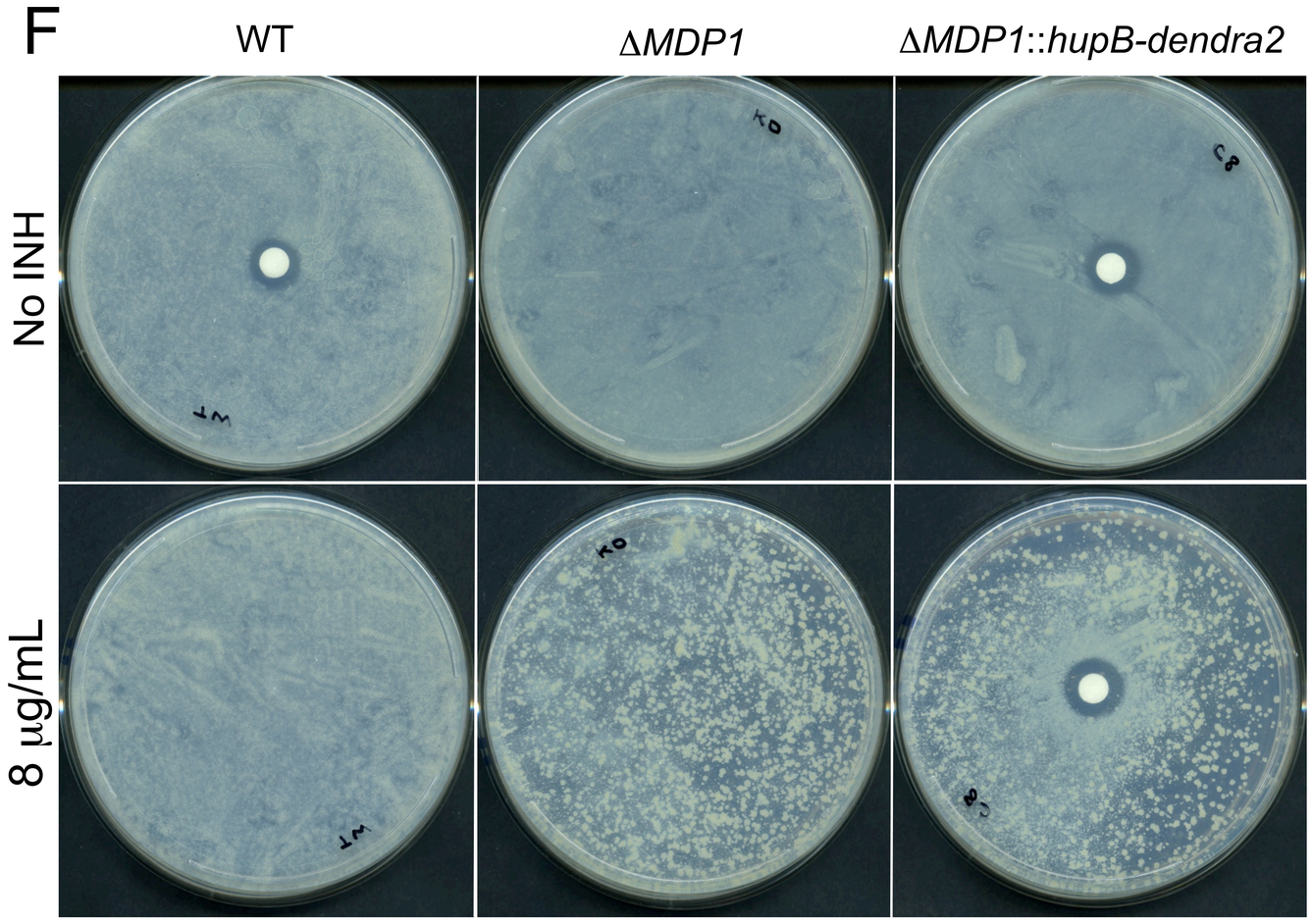

G

	WT	ΔMDP1	ΔMDP1::hupB-dendra2
No INH	Lawn	Lawn	Lawn
8 μg/mL	Lawn	Slow growing colonies	Near the disk, lawn; farther from the disk, slow growing colonies

Figure S2.

A H37Rv:

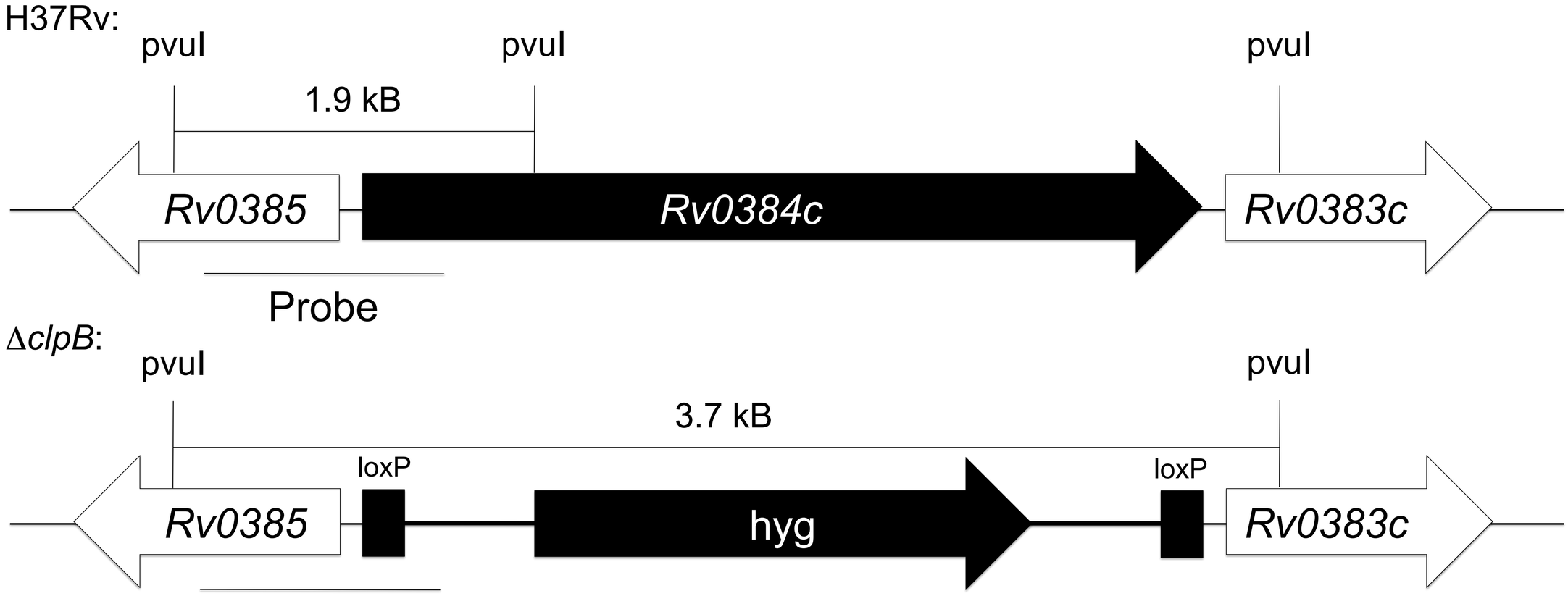

ΔclpB:

clpB-gfp:

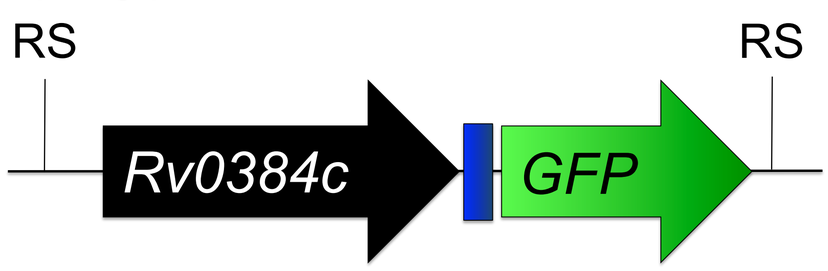

clpB-dendra2:

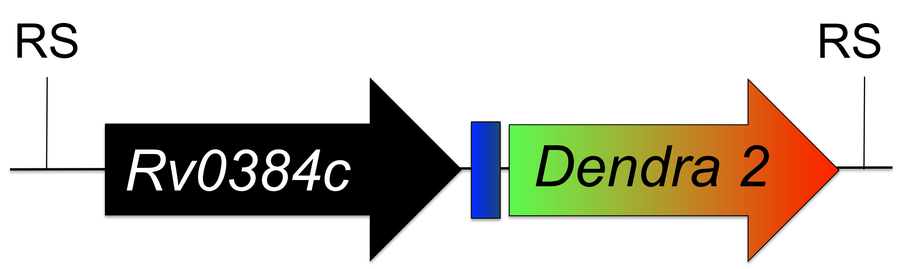

B Msm:

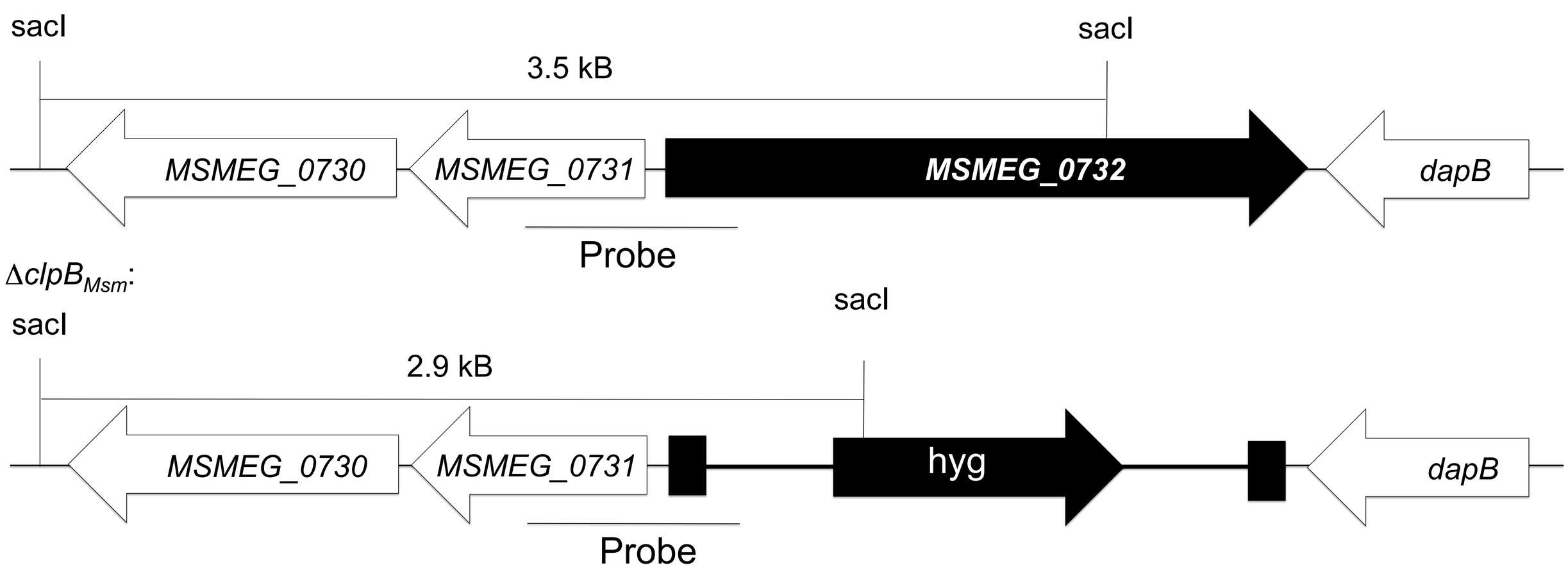

$\Delta clpB_{Msm}$:

C

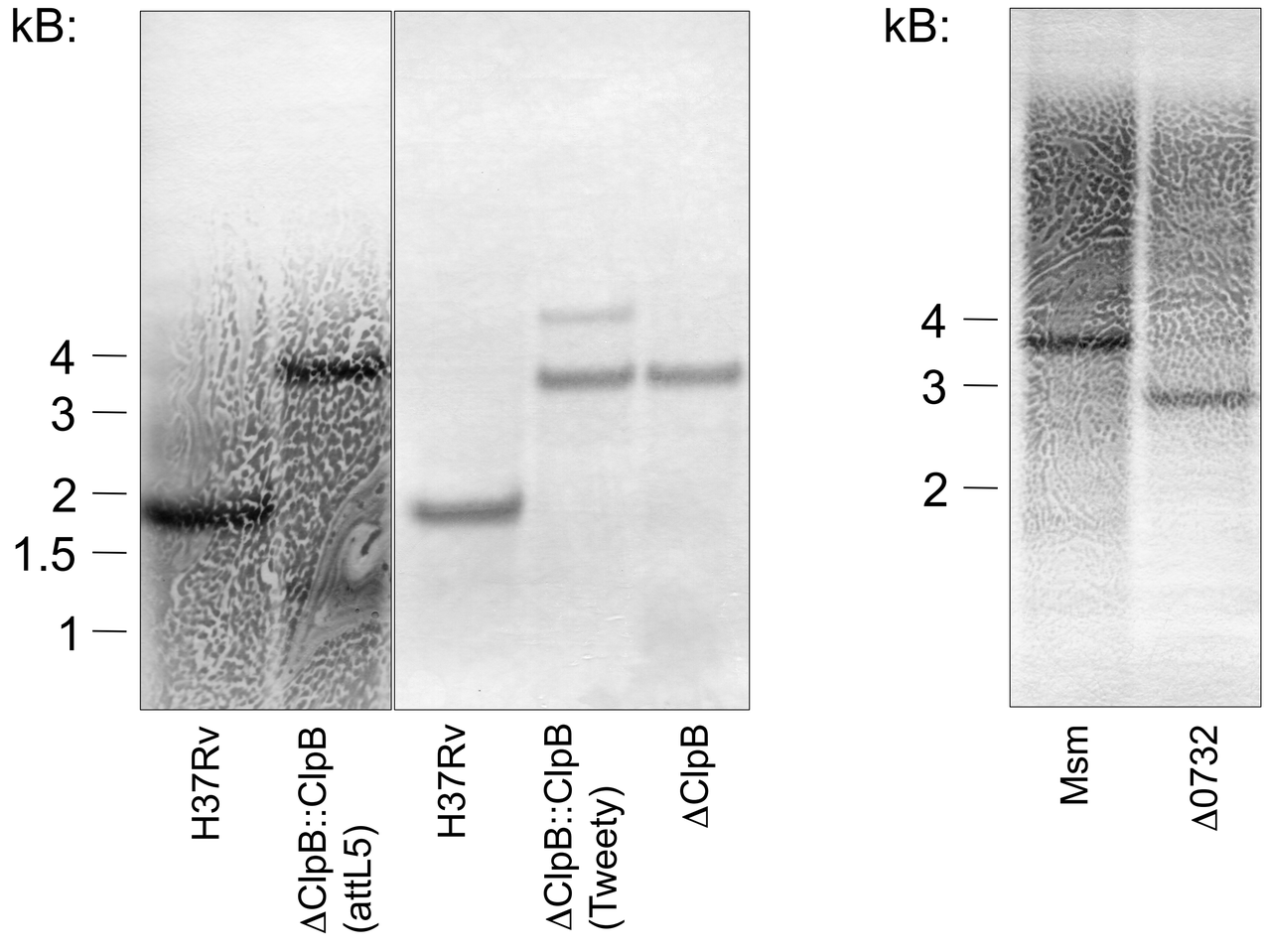

D

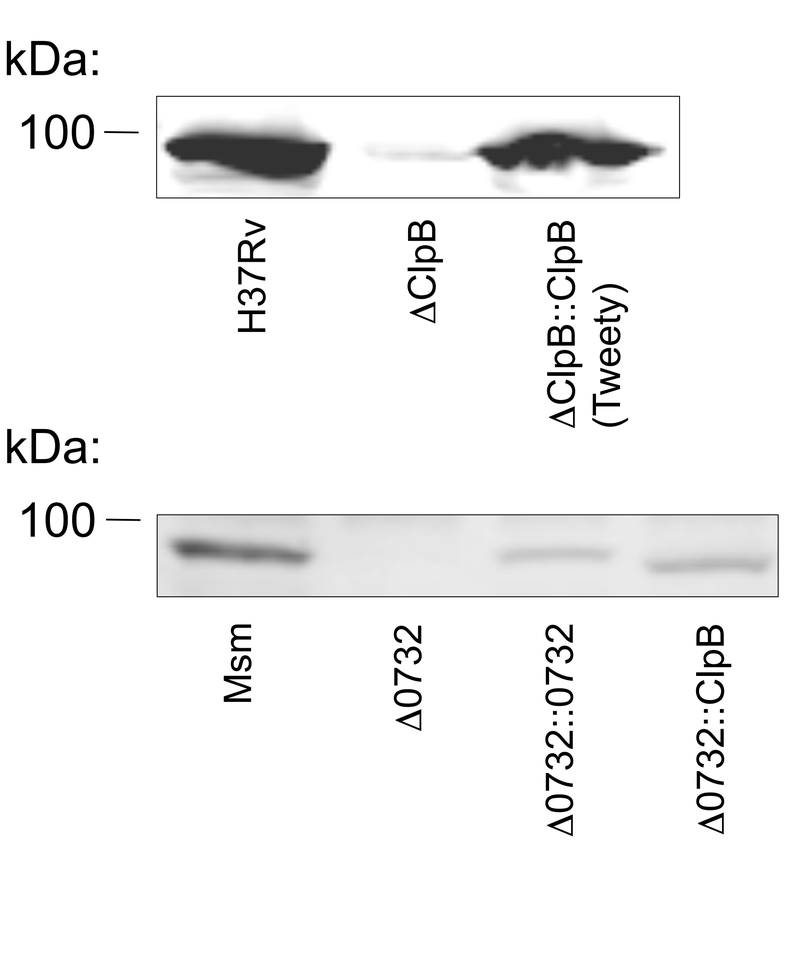

Figure S3.

A

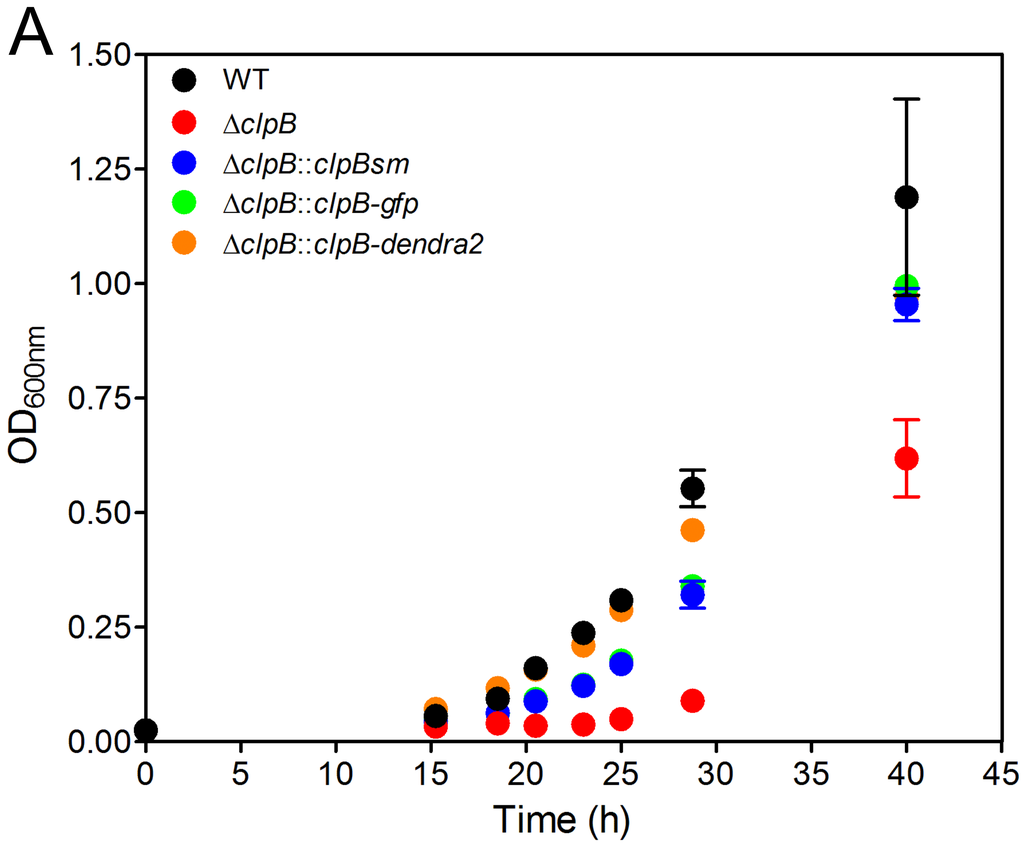

B

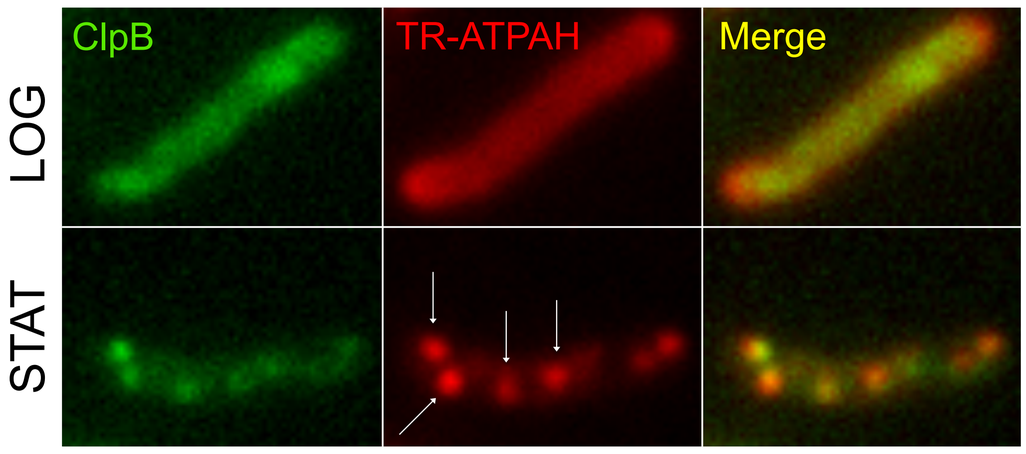

C

MNTPGINLIKEDMRVKVHMEGNVNGHAFVIEGEGKGK
PYEGTQTANLTVKEGAPLPFSYDILTTAVHYGNRVFTK
YPEDIPDYFKQSFPEGYSWERTMTFEDKGICTIRSDIS
LEGDCFFQNVRFKGTNFPPNGPVMQKKTLKWEPSTE
KLHVRDGLLVGNINMALLLEGGGHYLCDFKTTYKAKK
VVQLPDAHFVDHRIEILGNDSDYNKVKLYEHAVARYSP
LPSQVW

D

ATGAACACCCCGGGCATCAACCTGATCAAGGAGGACATGCGCGT
GAAGGTGCACATGGAGGGCAACGTGAACGGCCACGCCTTCGTGA
TCGAGGGCGAGGGCAAGGGCAAGCCGTACGAGGGCACCCAGAC
CGCCAACCTGACCGTGAAGGAGGGCGCCCCGCTGCCGTTCTCGT
ACGACATCCTGACCACCGCCGTGCACTACGGCAACCGCGTGTTC
ACCAAGTACCCGGAGGACATCCCGGACTACTTCAAGCAGTCGTTC
CCGGAGGGCTACTCGTGGGAGCGCACCATGACCTTCGAGGACAA
GGGCATCTGCACCATCCGCTCGGACATCTCGCTGGAGGGCGACT
GCTTCTTCCAGAACGTGCGCTTCAAGGGCACCAACTTCCCGCCG
AACGGCCCGGTGATGCAGAAGAAGACCCTGAAGTGGGAGCCGTC
GACCGAGAAGCTGCACGTGCGCGACGGCCTGCTGGTGGGCAAC
ATCAACATGGCCCTGCTGCTGGAGGGCGGCGGCCACTACCTGTG
CGACTTCAAGACCACCTACAAGGCCAAGAAGGTGGTGCAGCTGC
CGGACGCCCACTTCGTGGACCACCGCATCGAGATCCTGGGCAAC
GACTCGGACTACAACAAGGTGAAGCTGTACGAGCACGCCGTGGC
CCGCTACTCGCCGCTGCCGTCGCAGGTGTGG

E

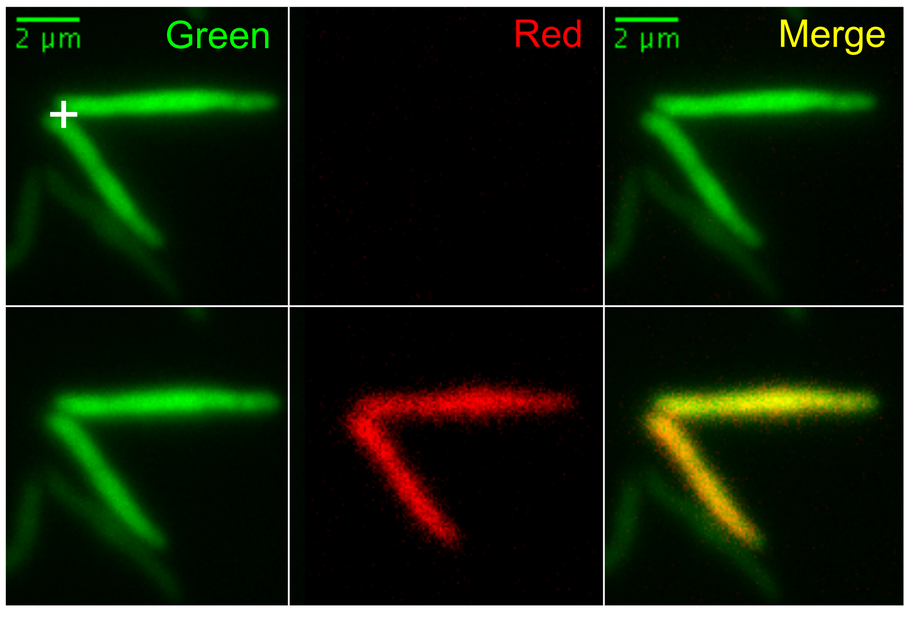

F

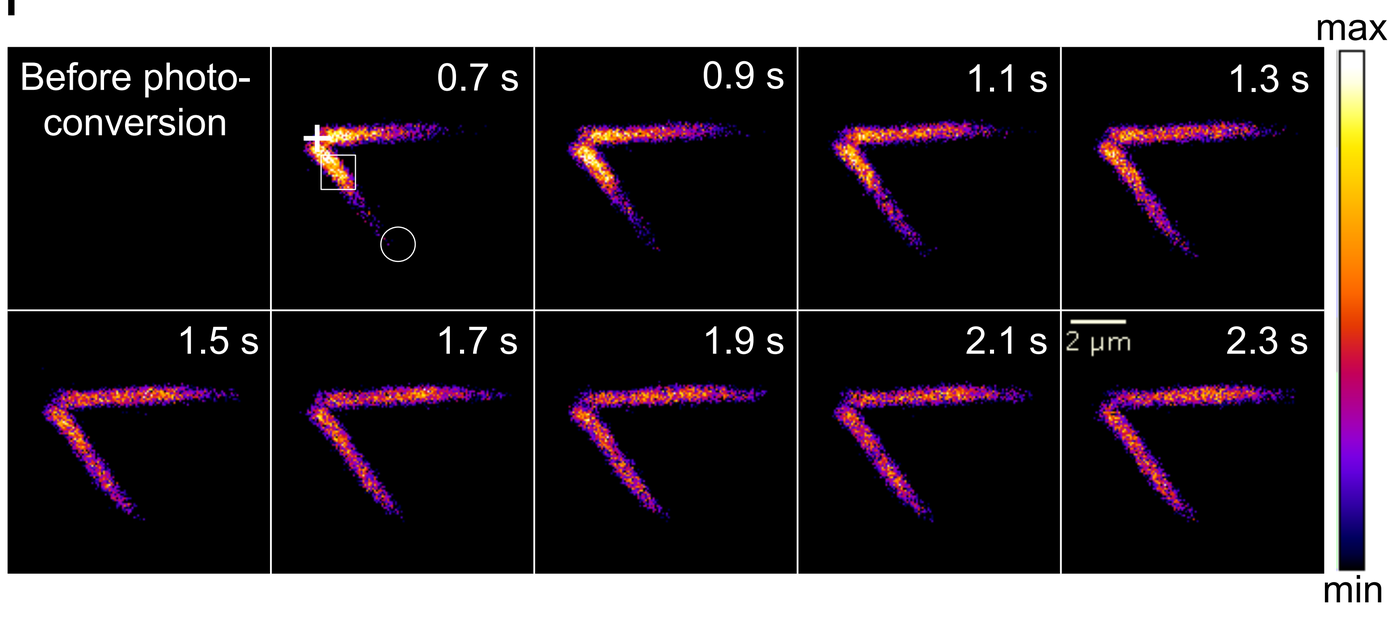

G

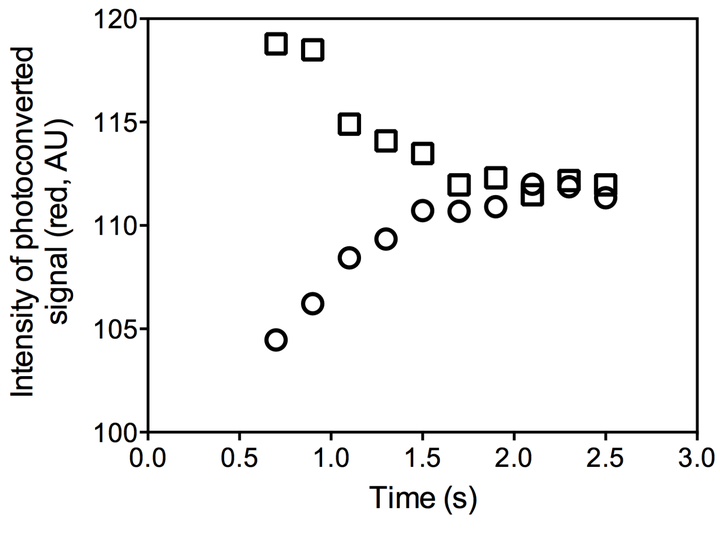

H

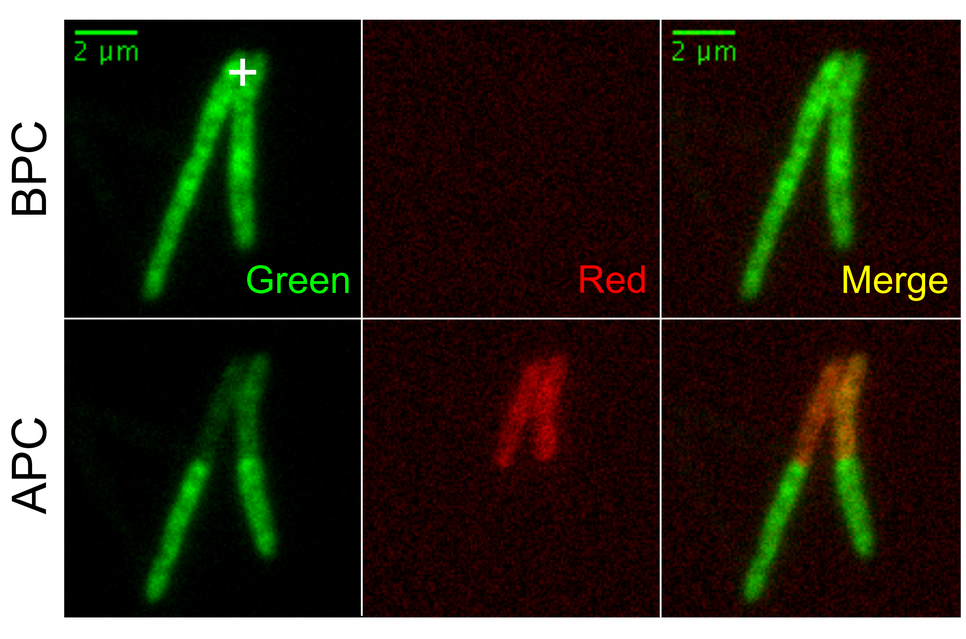

Figure S4.

A

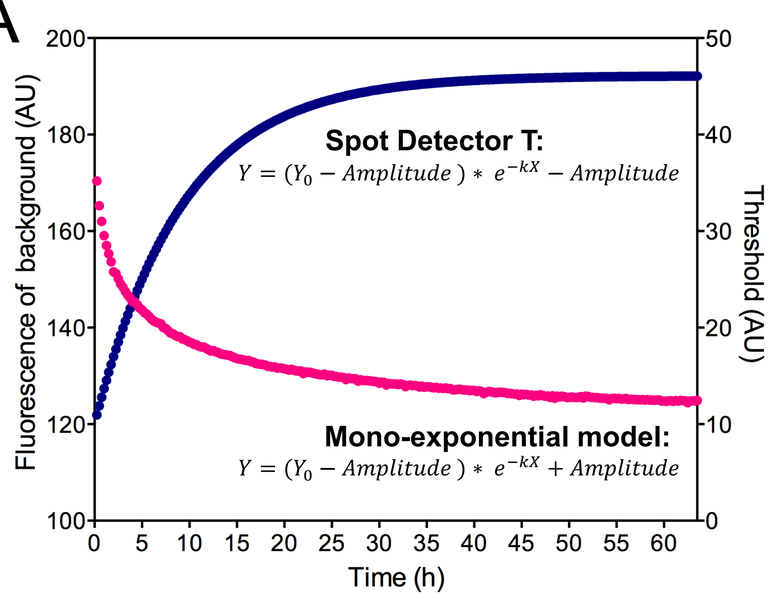

B

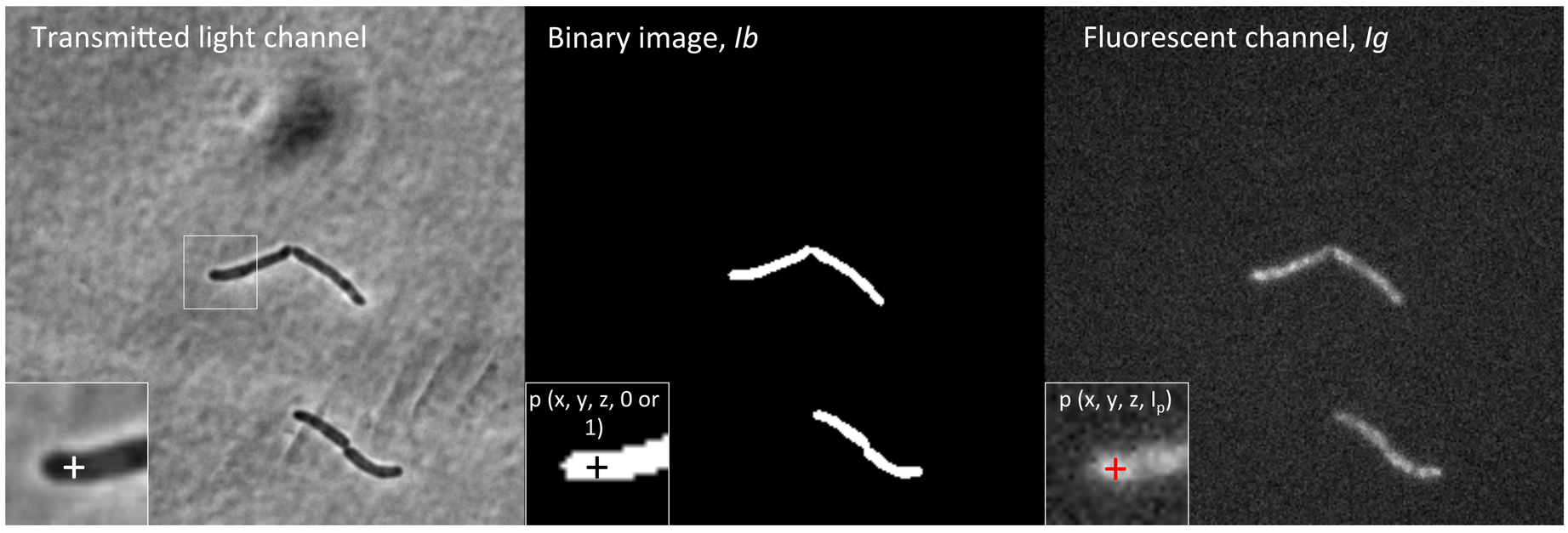

C

$$Area\ (A) = \sum_{x,y \in Ib; Ib(x,y)=1} Ib(x,y)$$

$$Mean\ Fluorescence\ Intensity\ (MFI) = \sum_{x,y \in Ib; Ib(x,y)=1} \frac{Ig(x,y)}{A}$$

$$Sum\ Fluorescence\ Intensity = \sum_{x,y \in Ib; Ib(x,y)=1} Ig(x,y)$$

$$Stddev\ Fluorescence = \sqrt{\frac{1}{A}\left(\sum_{x,y \in Ib; Ib(x,y)=1} Ig(x,y)^2\right) - MFI^2}$$

D

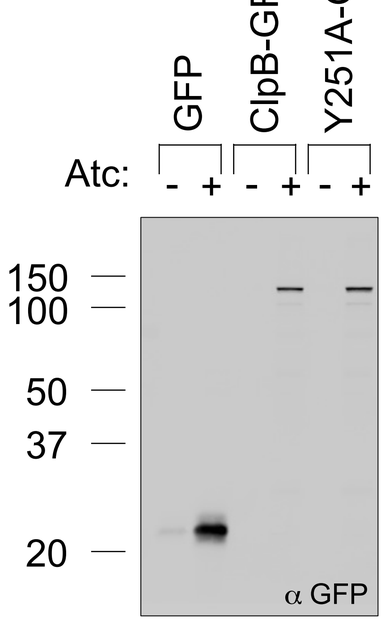

E

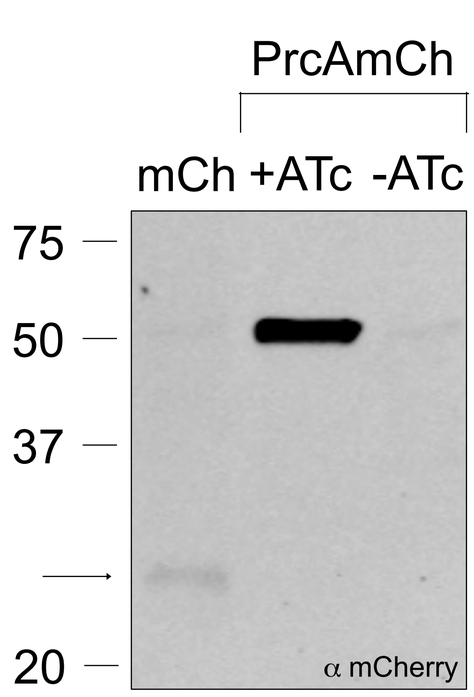

Figure S5.

A

Compounds	H37Rv	Δ*clpB*	Δ*clpB::clpB*
Kanamycin	2.5	2.5	2.5
Streptomycin	0.6	0.6-1.2	0.6-1.2
Isoniazid	0.2-0.4	0.2-0.4	0.2-0.4

MICs are in μg/mL. OD_{600nm} (inoculum) = 0.03

B

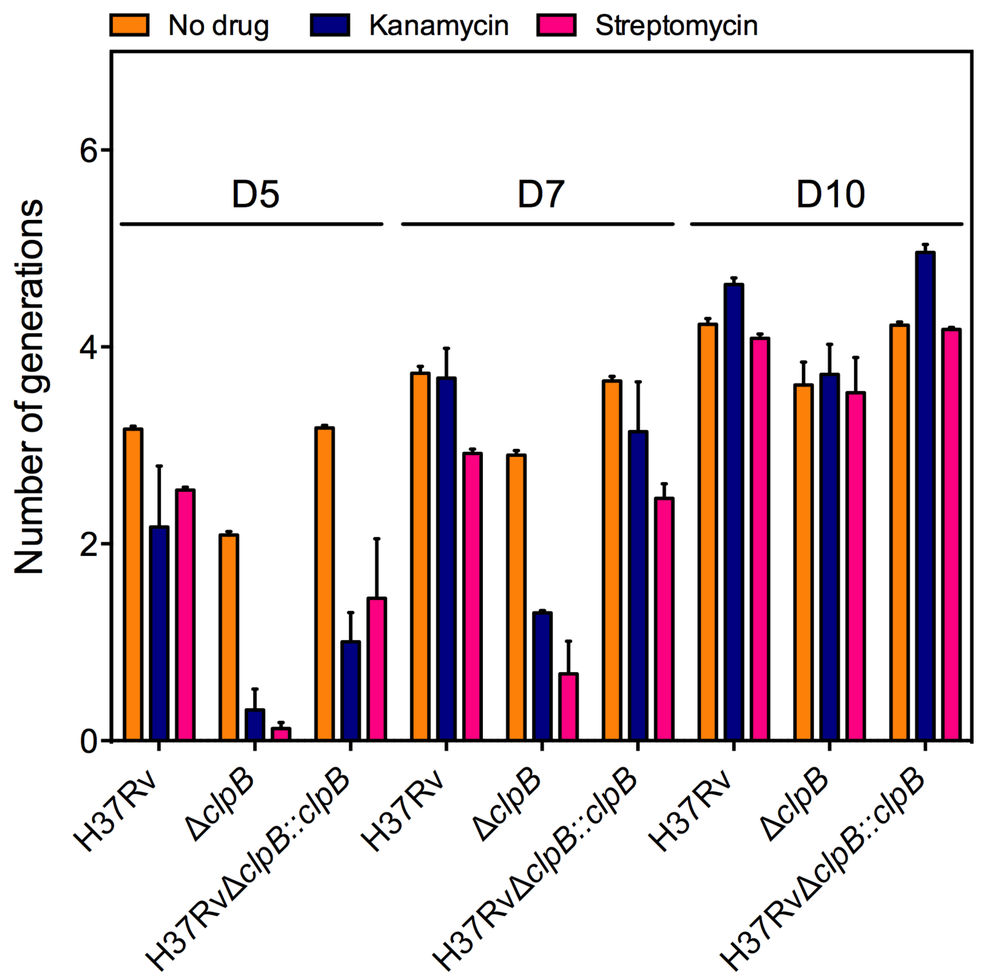

Figure S6.

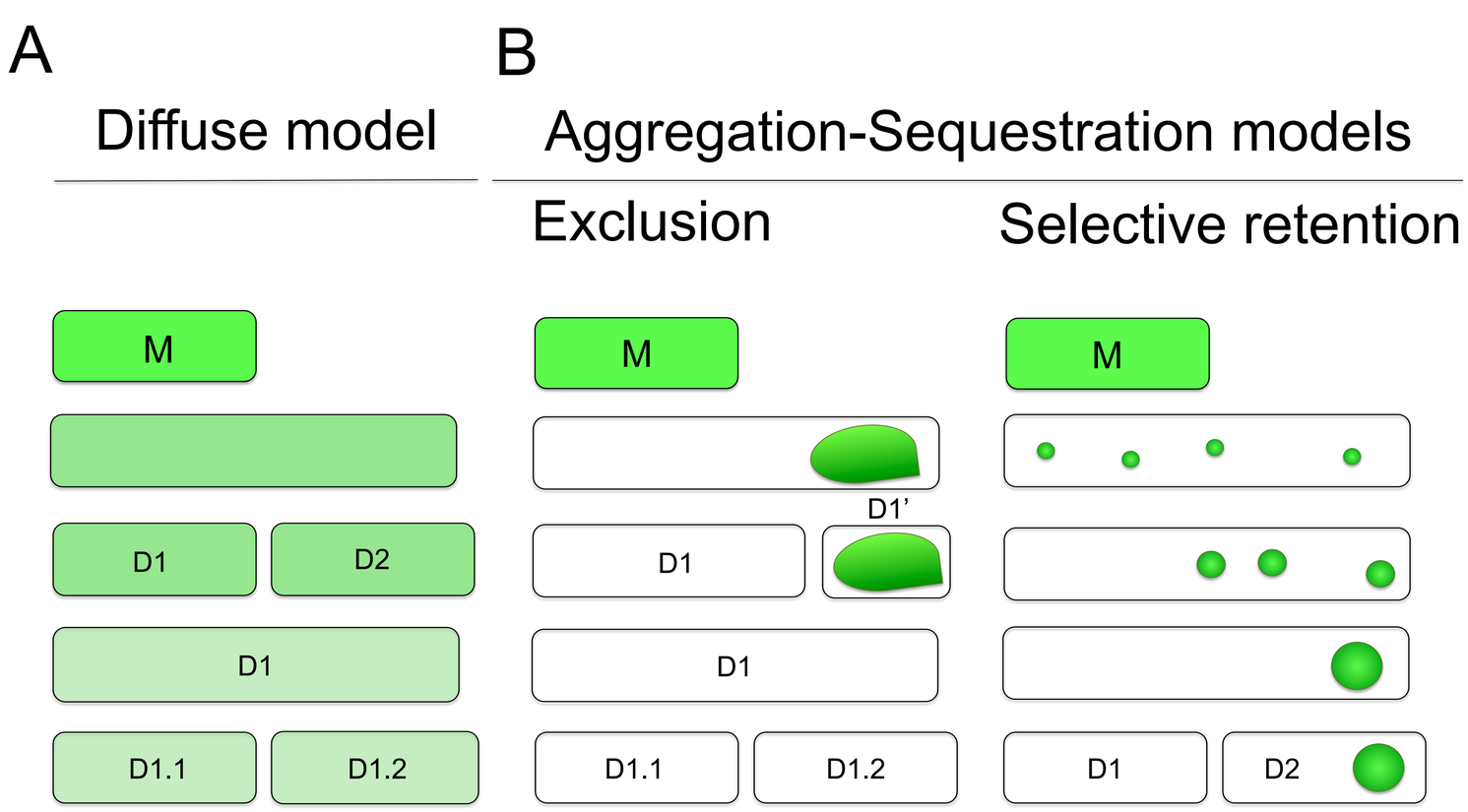
A
B
Diffuse model
Aggregation-Sequestration models
Exclusion
Selective retention
M
M
M
D1
D2
D1
D1'
D1
D1
D1.1
D1.2
D1.1
D1.2
D1
D2

Table S1:

ID #	Strains Name	Promoter [1]	Resistance [2]	Plasmid location [3]
1	*Mycobacterium smegmatis* (*Msm*)	N/A	N/A	N/A
2	*Mycobacterium tuberculosis* H37Rv (*Mtb*)	N/A	N/A	N/A
3	*Mtb*::pGMCS T10M-P1-*rv2986c-dendra2*	P_{myc1}*tetO*	S	C
4	*Msm*Δ*MSMEG_0732*::*hyg*	N/A	H	N/A
5	*Msm*Δ*MSMEG_0732*::*hyg*::*MSMEG_0732*	Native Msm	H & S	C
6	*Msm*Δ*MSMEG_0732*::*hyg*::*clpB*	Native Mtb	H & S	C
7	*Msm*Δ*MSMEG_0732*::*hyg*::*clpB-gfp (dubbed* Δ*clpBSm*::*clpB-gfp)*	Native Mtb	H & N	E
8	*Msm*Δ*MSMEG_0732*::*hyg*::*clpB-dendra2 (dubbed* Δ*clpBSm*::*clpB-dendra2)*	Native Mtb	H & N	E
9	*Mtb*Δ*clpB*::*hyg*	N/A	H & N & Z	N/A
10	*Mtb*Δ*clpB*::*hyg*::*clpB*	Native Mtb	H & N & Z	C
11	*Mtb*Δ*clpB*::*hyg*::*clpB-gfp*	Native Mtb	H & N & Z	C & E
12	*Msm*::pGMEN-10M-P1-*clpB-gfp*	P_{myc1}*tetO*	N	E
13	*Msm*::pGMEN-10M-P1-*clpBY251A-gfp*	P_{myc1}*tetO*	N	E
14	*Msm*::pGMEN-10M-P1-*gfp*	P_{myc1}*tetO*	N	E
15	*Msm*::pGMEN-0X-P38-*dendra2*	P38	N	E
16	*Msm*::pGMEN-0X-P38-*clpB-dendra2*	P38	N	E
17	*Msm*::pGMEH-10M-P1-*prcBA-mCherry*	P_{myc1}*tetO*	H	E

[1]: P_{myc1} (P1) and P38 are strong promoters. *tetO* (10M): expression depends on the addition of Atc.
[2]: Resistance: H, hygromycin; S, streptomycin; N, nourseothricin; Z, zeocin
[3]: Plasmid location: C, chromosomal; E, episomal
N/A: not applicable

Table S2:

ID #	Primers used for introducing genetic alterations
1 & 2	Not applicable
3	*attB2-SD-hupB:* GGGGACAGCTTTCTTGTACAAAGTGGCAGAAAGGAGGTTAATAATGAACAAAGCAGAGCTCATTGACGTGCTC *linker-hupB*: GCCCGAGCCCGAGCCCGATTTGCGACCCCGCCGAGCGG *linker-dendra2*: TCGGGCTCGGGCTCGGGCATGAACACCC *attB3r-dendra2*: GGGGACAACTTTGTATAATAAAGTTGCTATCACCACACCTGCGACGGCA
4	*attB1r-DMSMEG0732*: GGGGACTGCTTTTTTGTACAAACTTGTCACAGCAGGGGTGCGGCAATGCCGTCATTC *attB2-DMSMEG0732*: GGGGACAGCTTTCTTGTACAAAGTGGGTCCGCTGCGCCGGTTGGTGCAGCAG *attB3r-DMSMEG0732*: GGGGACAACTTTGTATAATAAAGTTGAGGACACCTGGATCGAGGTGGGTTACG *attB4-DMSMEG0732*: GGGGACAACTTTGTATAGAAAAGTTGGCCAGTTCCTGCTGATAGGCGTCAACC
5	as in (4) + *attB2-upDMSMEG0732*: GGGGACAGCTTTCTTGTACAAAGTGGTAGCCCTTACAGGCCCGGAGCAGCGGTGTTG *attB3r-DMSMEG0732*: GGGGACAACTTTGTATAATAAAGTTGTCAGCCCAAAACGAGGGACTCGC
6	as in (4) + *attB2-upClpB*: GGGGACAGCTTTCTTGTACAAAGTGGTCTAAGCTCGCGGCGAAACGGCGGCGGATGCA *attB3r-ClpB*: GGGGACAACTTTGTATAATAAAGTTGTCAGCCCAGGATCAGCGAGTCGGCGTCGGGGCTGA
7	as in (4) + *attB2-upClpB*: GGGGACAGCTTTCTTGTACAAAGTGGTCTAAGCTCGCGGCGAAACGGCGGCGGATGCA *linker-clpB:* ATGCCCGAGCCCGAGCCCGAGCCCAGGATCAGC *linker-pHGFP*: TCGGGCTCGGGCTCGGGCATGTCGAAGGGCGAG *attB3r-pHGFP*: GGGGACAACTTTGTATAATAAAGTTGGTTACTTGTACAGCTCGTCCATGCCGTGGGT
8	as in (4) + *attB2-upClpB*: GGGGACAGCTTTCTTGTACAAAGTGGTCTAAGCTCGCGGCGAAACGGCGGCGGATGCA *linker-clpB:* ATGCCCGAGCCCGAGCCCGAGCCCAGGATCAGC *linker-dendra2*: TCGGGCTCGGGCTCGGGCATGAACACCC *attB3r-dendra2*: GGGGACAACTTTGTATAATAAAGTTGCTATCACCACACCTGCGACGGCA
9	*attB1r-ClpB*: GGGGACTGCTTTTTTGTACAAACTTGTCACAGTAGCGGTGCGGCGATACCGTCGTTTT *attB2-ClpB*: GGGGACAGCTTTCTTGTACAAAGTGGCTGCAGGTCTCGCTGCCGGCCAAGCG *attB3r-ClpB*: GGGGACAACTTTGTATAATAAAGTTGATCTCCTGCGGCAGCGGCGGCAACACGC *attB4-ClpB*: GGGGACAACTTTGTATAGAAAAGTTGATCCGCCCGTTCGGGTCGGCCGGAATGGCT
10	as in (9) + *attB2-upClpB*: GGGGACAGCTTTCTTGTACAAAGTGGTCTAAGCTCGCGGCGAAACGGCGGCGGATGCA *attB3r-ClpB*: GGGGACAACTTTGTATAATAAAGTTGTCAGCCCAGGATCAGCGAGTCGGCGTCGGGGCTGA
11	as in (9) + *attB2-upClpB*: GGGGACAGCTTTCTTGTACAAAGTGGTCTAAGCTCGCGGCGAAACGGCGGCGGATGCA *linker-clpB:* ATGCCCGAGCCCGAGCCCGAGCCCAGGATCAGC *linker-pHGFP*: TCGGGCTCGGGCTCGGGCATGTCGAAGGGCGAG *attB3r-pHGFP*: GGGGACAACTTTGTATAATAAAGTTGGTTACTTGTACAGCTCGTCCATGCCGTGGGT
12	*attB2-SD-clpB*: GGGGACAGCTTTCTTGTACAAAGTGGCAGAAAGGAGGTTAATAGTGGACTCGTTTAACCC *linker-clpB:* ATGCCCGAGCCCGAGCCCGAGCCCAGGATCAGC *linker-pHGFP*: TCGGGCTCGGGCTCGGGCATGTCGAAGGGCGAG *attB3r-pHGFP*: GGGGACAACTTTGTATAATAAAGTTGGTTACTTGTACAGCTCGTCCATGCCGTGGGT
13	Same as (12) – primers to introduce mutations have been described in the method section
14	*attB2-SD-pHGFP*: *attB3r-pHGFP*: GGGGACAACTTTGTATAATAAAGTTGGTTACTTGTACAGCTCGTCCATGCCGTGGGT
15	*attB2-SD-dendra2*: GGGGACAGCTTTCTTGTACAAAGTGGCAGAAAGGAGGTTAATAATGAACACCCCGGGCATCAACC *attB3r-dendra2*: GGGGACAACTTTGTATAATAAAGTTGCTATCACCACACCTGCGACGGCA
16	*attB2-SD-clpB*: GGGGACAGCTTTCTTGTACAAAGTGGCAGAAAGGAGGTTAATAGTGGACTCGTTTAACCC *linker-clpB*: ATGCCCGAGCCCGAGCCCGAGCCCAGGATCAGC *linker-dendra2*: TCGGGCTCGGGCTCGGGCATGAACACCC *attB3r-dendra2*: GGGGACAACTTTGTATAATAAAGTTGCTATCACCACACCTGCGACGGCA
17	*attB2-SD-prcB*: GGGGACAGCTTTCTTGTACAAAGTGGCAGAAAGGAGGTTAATAGTGACCTGGCCGTTGCCCG *linker-prcA*: ATGCCCGAGCCCGAGCCCGAGCCCGACGATTCGCCGTCA *linker-mCherry*: TCGGGCTCGGGCTCGGGCATGGTGAGCAAGGGCGAGGA *attB3r-mCherry*: GGGGACAACTTTGTATAATAAAGTTGTCACTACTTGTACAGCTCGTCCATACCG

Extended Experimental Procedures

Oxidation of BSA

BSA (Fraction V, Roche) was dissolved at 10 mg/mL in 50 mM HEPES buffer, pH 7.4, supplemented with 100 mM KCl and 10 mM $MgCl_2$ (pre-oxidation buffer). Oxidation was achieved by incubation with freshly dissolved $FeCl_3$ and equimolar ascorbic acid at concentrations ranging from 25-100 mM (Maisonneuve et al., 2009) with continuous rotation for 16 hours at 37°C. Oxidation was stopped by addition of 1 mM ethylenediaminetetraacetic acid (EDTA), and samples were dialyzed at 4°C against pre-oxidation buffer with 1 mM EDTA. Protein concentration was determined using the bicinchoninic acid assay (BCA, Pierce).

Detection of carbonyls

Protein was extracted from mycobacteria in PBS containing a protease inhibitor cocktail (complete, Mini, Roche), 5% SDS and 50 mM DTT. 2,4-Dinitrophenylhydrazine (DNPH; 200 μl in 2M HCl) was added to 1 mL of a 1 mg/mL protein solution to achieve 1 mg/mL DNPH. After 1 hour at room temperature, trichloroacetic acid (TCA) was added (final concentration, 20%). After 30 min on ice, the suspension was centrifuged for 10 min at 750-1000 *g*. Pellets were washed 6 times with a mixture of 1:1 (v/v) ethanol:ethyl acetate, dissolved in PBS containing 5% SDS and separated on 10% SDS-Page gel (BSA) or 5% stacking gel (Mtb extracts) prior to immunoblotting using anti-DNP IgG (Bethyl Laboratories, Inc; dilution, 1:1000), or spectrophotometry at 371 nm. Anti-DNP IgG was probed using anti-goat IgG (IRDye® 680 Donkey Anti-Rabbit IgG, dilution, 1:10000; LI-COR Biosciences). Mtb's protein extracts require filtration for further processing outside of a BSL3 facility. We anticipated that this step could impair a full

recovery of IOP. As an alternative, we inactivated DNPH-treated samples by adding Laemmli sample buffer prior to heating to 100°C. This technical hurdle required the use of non-spectrophotometric methods but instead 5% stacking gel as described above. Alternatively, samples were resuspended in 0.1 M citric acid, 0.2 M Na_2HPO_4 (3:7, v/v), pH 6.4, and incubated with fluorescein-derivatized APTAH (132 μM) for 12 hours at 37°C with continuous rotation.

Identification of IOP

IOP were extracted as described in the previous section and captured using CarboLink™ Coupling Gel (Thermo Scientific) according to the manufacturer's instructions. Proteins covalently captured on beads were sequentially reduced with 10 mM dithiothreitol, alkylated with 100 mM iodoacetamide and digested with trypsin. Resulting peptides were collected, dried, dissolved in 0.1% formic acid in water, and separated by reverse phase using an Ultimate 3000 HPLC system connected to a LTQ-Orbitrap XL mass spectrometer (Thermo Scientific). Samples were trapped on a C18 trap column (5 μm ID beads, Thermo Scientific) at a flow rate of 30 $\mu l.min^{-1}$ prior to their separation using a customized C18 analytical column. Peptides were slowly eluted (flow rate of 0.5 $\mu l.min^{-1}$) using a 60 min gradient of solvents of decreasing polarity (buffer A, 0.1% formic acid in water and buffer B, 0.1% formic acid in acetonitrile). Mass spectra were recorded in a 400-1600 m/z mass range. MS scan resolution was set at a resolution of 30,000 for precursor and fragment ions. Eight precursors from each scan were selected for fragmentation. Fragments were acquired in profile mode. To resolve the less intense components of the samples, the dynamic exclusion method was applied using the following parameters: exclusion list size, 500; duration, 60 seconds; exclusion by mass with high and low exclusion mass widths of 1.5 ppm. The normalized collision energy in the ion trap was 35. Data were extracted and searched against the

Mycrobacterium tuberculosis Swissprot database using Mascot 2.3 (Matrix Science). All cysteines were considered alkylated with acetamide. Oxidation of methionine was allowed as a variable modification.

Cell fractionation

Cells were resuspended in PBS with protease inhibitor cocktail as above but without SDS and agitated with glass beads 0.5 mm, Cole-Parmer) (Precellys®24, Bertin Technologies or Mini-Beadbeater-1, Bio Spec Products Inc.) (5 times, 30 seconds with 2 min cooling intervals). Beads were removed by centrifugation for 15 seconds at 7500 *g* and unbroken cells were removed by centrifugation for 1 min at 7500 *g*. The second supernatant was centrifuged at 7500 *g* at 4°C for 1 hour. The final supernatant (soluble fraction) was collected and the sedimentable fraction was resuspended in a 3 M urea, 5% SDS.

Cross-linking

*Msm:*Δ*clpBsm*::*clpB-gfp* cells inoculated at low densities were grown to an OD_{600nm} of 0.25. Kanamycin was added (1 μg/mL) to separate cultures for 30 or 90 minutes. Cells were collected by centrifugation at 3000 *g* for 8 min, washed once with PBS and resuspended in 1 mL of PBS containing 1 mM of disuccinimydyl glutarate (DSG, Thermo Scientific) for 30 minutes. Cells were washed once with PBS and resuspended in PBS supplemented with 50 mM Tris. Cells were washed, resuspended in PBS containing 5% SDS and protease inhibitor cocktail and subjected to bead beating. Protein concentration was measured using *DC*™ Protein Assay (Biorad). Protein extracts (70 mg protein) were separated by 10% SDS PAGE, and transferred to a nitrocellulose membrane for immunoblotting with anti-GFP mAb.

Antibodies to ClpB, GFP and mCherry and antiserum to ClpB

Recombinant His-tagged ClpB from Mtb was purified as reported (Werbeck et al, 2008) except for the final concentration step, which was performed using a Centricon filter (EMD Millipore) and used to immunize rabbits with Freund's incomplete adjuvant. ClpB antiserum and ClpB antibodies were used at dilution 1:1000 and 1:2500, respectively. Green Fluorescent Protein (GFP) and mCherry monoclonal antibodies were from Clontech (Living colors® Av, JL-8, 1:8000; Living colors® mCherry Av, 1:1000).

Genetic alterations

Plasmids were constructed with Gateway® Cloning Technology (Life Technologies). Before fusion to HupB and ClpB, *dendra2* was adapted to mycobacterial codon usage with the Codon Adaptation Tool at www.jcat.de. Codon-adapted *dendra2* was synthesized, cloned into a pUC57 vector (GenScript Corporation) and amplified using primers containing *attB* sites (*attB2*, ggggacagctttcttgtacaaagtgg; *attB3r*, ggggacaactttgtataataaagttg) for integration by recombination into Gateway® vectors. Dendra2 was expressed episomally under a strong, constitutive promoter (P38) in *Msm* for proof of principle experiments to assess conditions of photoconversion. We used Dendra2 both for its spectral properties and to reduce the concern that certain fluorescent reporters can cause mislocalization when fused to homo-oligomers (Landgraf et al., 2012).

To construct *Msm:*Δ*MSMEG_0732*::*hyg* deletion mutants, we transformed Msm with a temperature-sensitive plasmid pXSTS *upMSMEG_0732*-hygR-*doMSMEG_0732*, which contains regions upstream and downstream of *MSMEG_0732*, flanking a *hyg* resistance cassette. Transformants were selected on 7H11 plates supplemented with 0.5% glycerol

and 50 μg/mL hygromycin, incubated in a chamber maintained at 37°C. Transformants' XylE-activity was verified by addition of 20 μL of a solution of 2% catechol (Pyrocatechol ≥99%, Sigma-Aldrich), which turned colonies yellow. Transformants were inoculated in 5 mL of 7H9 supplemented with 50 μg/mL hygromycin and incubated at 37 °C until cultures reached an OD 600_{nm} of 1. For each transformant, 100 μL of the culture were plated on 7H11 agar containing 50 μg/mL hygromycin. Ten plates per transformant were incubated in a chamber maintained at 40 °C to select for transformants that lost the temperature-sensitive plasmid. Colonies that emerged were assessed for their XylE activity. Those that presented no XylE activity were cultured in 7H9 medium and candidates validated by Southern blot.

To construct *Mtb:*Δ*clpB*::*hyg*, we integrated a second copy of *clpB (Rv0384c)* alongside ClpB's upstream region using a plasmid pGMCS-*upRegclpB* that integrates in the attachment site for the mycobacteriophage L5 (att-L5). *upReg* stands for upstream region that contains Clp's native promoter. We integrated a PCR product into the genome of this merodiploid strain by phage-mediated recombineering (van Kessel and Hatfull, 2007). We cloned a plasmid that contained sequences homologous to the regions upstream (*upclpB*) and downstream (*doclpB*) of *clpB,* flanking a *hyg* resistance cassette. From this plasmid, we amplified the substrate for recombination, *upclpB*-hygR-*doclpB,* using the primer pair REC_clpBup (ACCGCTCATCACCCCGATGATCAGG) and REC_clpBdown (GTCTAGATTGGTGGAGTACACCATCCGT). We transformed *Mtb*::pGMCS-*upclpB*-hygR-*doclpB*::pNit-recET-sacB-kan cells with 500 ng of the PCR fragment. 12 $Strep^R$ Hyg^R Kan^R colonies were inoculated into 24-well plates containing 1 mL of 7H9 supplemented with appropriate antibiotics. When densities of ~ 0.8-1 OD were reached, glycerol stocks were prepared and culture volumes were expanded. Merodiploid candidates were validated by Southern blot. For two merodiploid strains, the

native copy of *clpB* was deleted from the attL5 site by replacement with an empty vector. This strain was passaged in absence of kanamycin to eliminate the pNit-recET-sacB-kan plasmid; the resulting strain was *Mtb:*D*clpB*::*hyg* (ID # 9, Table S1). *Mtb:*D*clpB*::*hyg* was further transformed with a plasmid that inserts *clpB* and *clpB*'s upstream region in the tweety site, producing *Mtb:*D*clpB*::*hyg*::*clpB (*ID # 10, Table S1). A mutation of ClpB was introduced by PCR to effect Tyr-to-Ala substitution at amino acid 251. To do so, a set of 2 primers pairs were used: *attB2-clpB,*GGGGACAGCTTTCTTGTACAAAGTGGCAGAAAGGAGGTTAATAGTGGACTCGT TTAACCC and *Y251Arev* (*Y251Arev*: CTCGAATTCGCCGCGGGCTTTGGAGCCGGCGACCAT) and *attB3r-clpB* GGGGACAACTTTGTATAATAAAGTTGGTTACTTGTACAGCTCGTCCATGCCGT and *Y251Afor* (*Y251Afor*: GGTCGCCGGCTCCAAAGCCCGCGGCGAATTCGAG). These PCR fragments were used for further Gateway® cloning. Reporter constructs fused GFP, mCherry or Dendra2 to the C-terminus of the indicated protein. The nucleotide sequence tcgggctcgggctcgggc encoding the linker SGSGSG was introduced between the nucleotide sequences encoding the protein of interest and the reporter. As indicated in Table S1, expression was either constitutive (0X) or regulated (native regulation or regulation by the addition of anhydrotetracycline acting via TetR). A plasmid was constructed for Atc-inducible expression of *prcB* (*Rv2110c*), *prcA* (*Rv2109c*) and *mCherry,* as verified by western blot.

For verification by Southern blot, 10 to 20 μg of genomic DNA of *Msm:*Δ*MSMEG_0732*::*hyg*, the merodiploid strain, *Mtb:*Δ*clpB*::*hyg*, and *Mtb:*Δ*clpB*::*hyg*::*clpB* was digested with *SacI (*Msm:Δ*MSMEG_0732*::*hyg)* and PvuI (Mtb's strains). DNA fragments were probed using labeled PCR products. The primer pairs were CCGACGACGTAGCTGACCCG and

CTGAGTCTTGGTCGTCGGGTTGAACGAGTCC for Msm and TCTGGCGCACGTGCAGACCG and CTTGGTCGTCGGGTTAAACGAGTCCAC for Mtb. The expected sizes of the fragments detected were 3517 base pairs (bps) for Msm and 2878 bps for Msm:Δ*MSMEG_0732*::*hyg*. For Mtb strains, the following sizes were anticipated: Mtb, 1836 bp; merodiploid, 1140 and 3730 bp; Mtb::Δ*clpB*::*hyg*, 3730 bp; Mtb::Δ*clpB*::*hyg*::*clpB*, 3730 bp and 4984 bps. Hybridization was detected using an ECL chemoluminescent system (GE Healthcare) according to the manufacturer's instructions.

Synthesis of rhodamine 101 sulfonamido-PEG(4)-hydrazide, 4 and fluorescein sulfonamido-PEG(4)-hydrazide, 7.

Texas red derivative **4** was synthesized starting from sulforhodamine 101, **1,** which was first converted to the sulfonyl chloride (Romieu et al., 2008) with a large excess of neat phosphorous oxychloride. After vacuum evaporation of $POCl_3$, the crude sulfonyl chloride was directly reacted with N-Boc-protected hydrazidocarbonyl-PEG(4) amine, **2,** in the presence of triethylamine (TEA) in dry DMF to give protected hydrazide **3** in 60% yield. Boc group removal by treatment with TFA (100 equiv.) in CH_2Cl_2 provided the rhodamine 101 sulfonamido-PEG(4)-hydrazide, **4**.

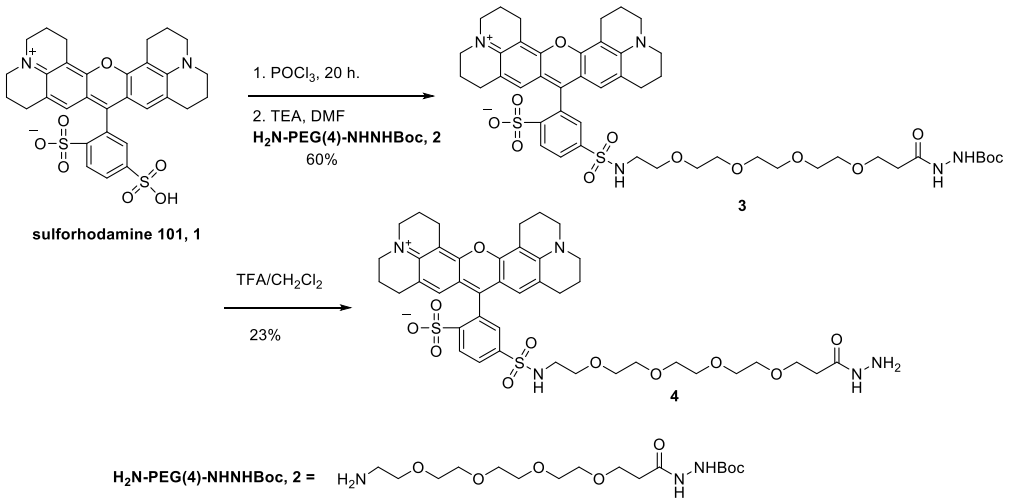

The fluorescein derivative **7** was synthesized starting from commercial 9-fluorescein isothiocyanate **5** (Meijler et al., 2005). Reaction of **5** with H_2N-PEG(4)-NHNH-Boc **2** in the presence of DIPEA in dry DMF afforded the desired thiourea, **6**. After removal of *t*-butyl carbonyl group by treatment with TFA (100 equiv.) in CH_2Cl_2, the fluorescein hydrazide **7** was obtained as an orange solid.

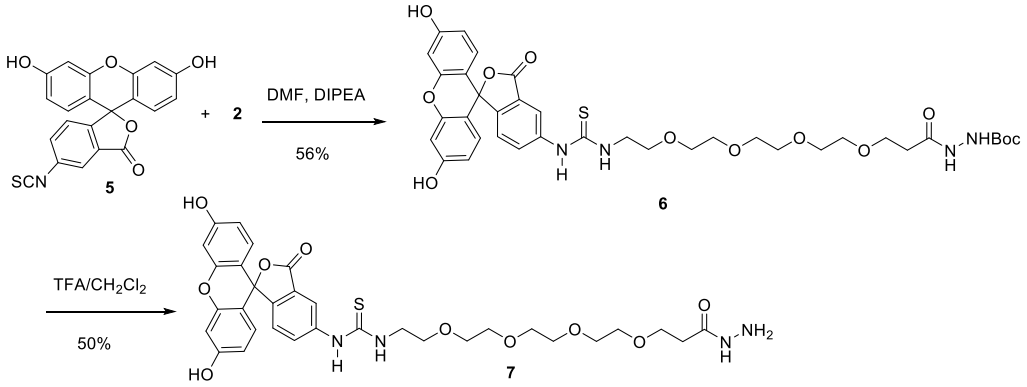

Chemical and Reagents. Sulforhodamine 101 **1** and Fluorescein 5-isothiocyanate **5** were purchased from Sigma-Aldrich. H_2N-PEG(4)-NHNH-Boc **2** was from Iris Biotech GmbH. The anhydrous solvents were from Sigma-Aldrich and were used without further processing. All reactions were performed under an atmosphere of pre-purified argon.

Instruments. ^{1}H NMR spectra were recorded on a Bruker AVANCE DRX-500 (500 MHz) spectrometer at 24 °C. Low-resolution mass spectra were performed on an AB-Sciex 100 mass spectrometer using electrospray ionization. Analytical TLC was performed on E. Merck silica gel 60 F254 plates and flash column chromatography was performed on Teledyne-Isco Combi Flash, using pre-packed columns. HPLC separations involved a mobile phase of 0.005% TFA (v/v) in water (solvent A)/0.005% TFA in acetonitrile (solvent B). Analytical LC-MS analyses were performed on an Acquity^{TM} UPLC-MS from Waters equipped with Acquity UPLC® BEH C18, 1.7 µm, 2.1 x 100 mm column at a flow rate of 0.3 mL/min. Preparative separations were performed using an Autopure preparative HPLC system equipped with a Waters 2998 PDA detector and 3100 mass detector and XBridge Prep. C18 reverse phase HPLC column 5 µm, 19 x 150 mm at a flow rate of 20.0 mL/min.

Experimental Procedures: Preparation of *N*-sulforhodamine 101-PEG(4)-tert-butyl hydrazide **3**. Sulforhodamine 101 (20 mg, 0.033 mmol) was dried under high vacuum for 2 h. The resulting powder was mixed with 125 µL of neat phosphorus oxychloride (1.36 mmol). The mixture was stirred at room temperature under an argon atmosphere for 20 h. Thereafter, $POCl_3$ was removed under vacuum, and the residue was dried under high vacuum at room temperature for 1 h. To the above flask, a solution of H_2N-PEG(4)-NHNH-Boc (25 mg, 0.066 mmol) and TEA (25 µL, 0.165 mmol) in dry DMF (2 mL) was added at 0 °C. The resulting mixture was protected from light and was stirred at room temperature under an argon atmosphere overnight. The reaction was checked for completion by UPLC (C18 column, 45-55% CH_3CN/H_2O with 0.005% TFA). Upon completion, the reaction mixture was diluted in CH_2Cl_2 (20 mL) and washed with deionized water (20 mL). The organic layer was dried over anhydrous Na_2SO_4 and purified by Teledyne-Isco Combi flash chromatography on a 4.0 g silica gel column using

10% methanol in CH_2Cl_2 as eluant to give 23 mg of *tert*-butylcarbonyl hydrazide **3** (60 %). MS (ESI, positive mode): calcd for $C_{47}H_{61}N_5O_{13}S_2Na$ exact mass 990.36 $[M+Na]^+$, found 990.6.

Removal of *tert*-butyl carbonate. The above *N*-Boc hydrazide **3** (20 mg, 0.02 mmol) was dissolved in CH_2Cl_2 (2 mL) and cooled to 0 °C, at which temperature TFA (400 μL) and deionized water (10 μL) were added. The resulting reaction mixture was warmed to room temperature and stirred for 2h. Upon completion (UPLC: C18 column, 20-60% CH_3CN/H_2O with 0.005% TFA), the mixture was evaporated to dryness. TFA removal was further insured by repeated azeotropic distillations with toluene (2 x 1 mL). The resulting residue was then dissolved in water and acetonitrile and submitted to preparative RP-HPLC (C18, eluting with 47-50 % CH_3CN/H_2O gradient containing 0.005% TFA) to afford 6 mg of hydrazide **4** as a red powder (23% yield, not optimized). ^1H NMR (500 MHz, Methanol-d4): δ 8.56 (s, 1H), 8.02 (d, *J* = 7.8 Hz, 1H), 7.36 (d, *J* = 7.9 Hz, 1H), 6.53 (s, 2H), 3.68 (t, *J* = 5.7 Hz, 2H), 3.66-3.45 (m, 18 H), 3.41 (t, *J* = 5.3 Hz, 4H), 3.16 (t, *J* = 5.2 Hz, 2H), 2.98 (m, 4H), 2.62-2.56 (m, 4H), 2.45 (m, 2H), 2.01(m, 4H), 1.85 (m, 4H). MS (ESI, positive mode): calcd for $C_{42}H_{54}N_5O_{11}S_2$ exact mass 868.33 $[M+H]^+$, found 868.6.

Synthesis of probe **7**. A solution of H_2N-PEG(4)-NHNH-Boc **2** (20 mg, 0.052 mmol) in DMF (1 mL) was treated with FITC **5** (23 mg, 0.06 mmol) and DIPEA (175 μL, 1.00 mmol) and stirred at room temperature for 16 h. DMF was then removed under high vacuum at room temperature, and the resulting orange residue was taken up in CH_2Cl_2. Flash chromatography using 5-10 % (v/v) MeOH in CH_2Cl_2 afforded 20 mg (50 %) of *N*-Boc hydrazide **6**. MS (ESI, positive mode): calcd for $C_{37}H_{44}N_4O_{12}SNa$ exact mass 791.26 $[M+Na]^+$, found 791.4.

Final deprotection. The above *N*-Boc hydrazide **6** was dissolved in CH_2Cl_2 (2 mL) and cooled to 0 °C. TFA (300 μL) and deionized water (10 μL) were added through syringe, and the resulting reaction mixture was warmed to room temperature and stirred for 2 h. Reaction progression was monitored by UPLC (C18 column, 20-60% CH_3CN/H_2O with 0.005% TFA), and upon completion, the mixture was evaporated to dryness. Complete TFA removal was further insured by azeotropic distillation with toluene (2 x 1 mL). The resulting residue was dissolved in water and acetonitrile and submitted to preparative RP-HPLC (C18, eluting with 25-50% CH_3CN/H_2O with 0.005% TFA) to afford 16 mg of desired hydrazide **7** (50%) as an orange powder. ^{1}H NMR (500 MHz, Methanol-d4): δ 8.14 (s, 1H), 7.74 (d, *J* = 7.6 Hz, 1H), 7.10 (d, *J* = 8.2 Hz, 1H), 6.75 (d, *J* = 8.8 Hz, 2H), 6.70 (d, *J* = 2.0 Hz, 2H), 6.56 (dd, *J* = 2.1, 8.6 Hz, 2H), 3.72 (br s, 2H), 3.63 (m, 4H), 3.58 (s, 4H), 3.52 (m, 4H), 3.49 (s, 4H), 2.43 (t, *J* = 5.6 Hz, 2H). MS (ESI, positive mode): calcd for $C_{32}H_{37}N_4O_{10}S$ exact mass 669.22 $[M+H]^+$, found 669.4.

Confocal fluorescence and time-lapse microscopy

Strains that expressed GFP, Dendra2 or mCherry or that were labeled using fluorescent chemical probes (APTAH, 25 mM; Hoescht, 5 mM, Invitrogen) were visualized using an inverted Olympus IX-70 microscope equipped with appropriate filter sets, a Photometrics CoolSnap QE cooled CCD camera, and an Insight SSI 7 color solid state illumination system. For photoconversion, a 410 nm laser was applied to the targeted area for 100 to 500 ms at a 10-30% power. Mtb was fixed with 4% paraformaldehyde for 4 hours before imaging outside of a biologic safety level 3 facility. Cells that were not subjected to time-lapse photomicroscopy were mounted between slides and coverslips using ProLong® Gold Antifade (Life Technologies). For time-lapse studies, bacteria were grown to mid-log phase (OD_{600} ~0.5) in 7H9 medium, collected by centrifugation (2400 *g*, 5 min),

concentrated 10-fold in fresh 7H9 medium (37 °C) and passed through a 5-µm pore size PVDF syringe filter (Millipore) to remove clumps. The cell suspension was spread on a semi-permeable membrane (Pectra/Por7 25 KD, Spectrum Laboratories), inverted on a coverslip, placed in the custom-built microfluidic device described by Wakamoto et *al.* and Santi et *al*. and continuously perfused with 7H9 medium at 37 °C (Santi et al., 2013; Wakamoto et al., 2013). Mycobacteria taken from flask cultures were allowed to adapt in the microfluidic device until they elongated with a velocity of ~ 1 $\mu m.h^{-1}$ (Santi et al., 2013). Elongating and dividing bacteria formed microcolonies that were imaged every 10-15 minutes using a DeltaVision personal DV inverted fluorescence microscope (Applied Precision) mounted with a 100x oil immersion objective in an environmental chamber at 37 °C. When indicated, the perfusate was supplemented with an antibiotic. Images were recorded on transmitted light and fluorescence channels (for GFP or Dendra2, excitation filter 490/20, emission filter 528/38; for mCherry, excitation filter 575/25, emission filter 632/60) using a CoolSnap HQ2 camera.

Computational palette

We customized the SpotDetector plugin hosted by the open source image analysis software Icy (de Chaumont et al., 2012). Spots were detected using an undecimated wavelet transform detector, modified by introduction of continuous threshold modulation scaled to an ascending mono-exponential to compensate for the time-dependent loss of fluorescence caused by photo-bleaching during sequential observations (Figure S5A). In this study, spots are therefore defined as pixel-made objects, for which the wavelet coefficients correlate across successive resolution levels (Olivo-Marin, 2002). Practically, this allowed their detection despite their heterogeneity in size and intensity. Next, we developed two open-source de-noising algorithms to study bacterial phenotypes at the

population scale. First, we designed an automatic segmentation software for analyzing time-lapse sequences of transmitted-light images of microcolonies, which relies on successive algorithms to accurately and robustly identify bacterial location in the imaged field in the presence of artifacts, such as particulate material. The initial step consisted in enhancing coefficients corresponding to bacterial edges in a mathematical space dedicated to image representation and subsequently reconstructing a feature-enhanced image (Unser and Chenouard, 2013). This enhanced bacterial contours and eliminated stochastic artifacts and noise. A mask of a microcolony was obtained by applying a threshold to the value of the enhanced image's pixels and grouping them into clusters. To eliminate elongated artifacts with edge-like structures, a last step evaluates the values of neighboring pixels of each candidate bacterium. Only structures surrounded by a halo, a signature of mycobacteria imaged by transmitted-light microscopy, qualified for definition as bacteria. The whole-image analysis procedure, termed MycoMask, was implemented as a plug-in for ICY. This plugin does not require human intervention so that reproducible and unbiased results are obtainable for a large quantity of data, favoring statistical significance and robustness. In heavily clumped microcolonies, mycobacteria that are not at the edge of the cluster often fail to display a halo identifiable by transmitted-light microscopy. Thus, we developed a second plugin that shares initial steps with those of MycoMask but replaced the last algorithm with a multi-step procedure. We apply a dedicated morphological operator to fill holes in the binary pre-mask of bacteria. Morphological closing is applied to the pre-mask alongside pixels corresponding to halos typical of bacteria edges to improve the outline of the microcolony. A size criterion then identifies clusters of otherwise undetected pixels inside the outline of the bacterial mask, mostly corresponding to regions displaying poor contrast due to bacterial clumping. The procedure is implemented as a plugin—Mycoclump—for the open-source image analysis software ICY. For single-cell analysis,

we used manual segmentation assisted in some cases by the Bacterial Image-Sequence QUantification Interactive Tool (BisQuit), a plugin hosted by ImageJ that allows semi-automated and interactive analysis of image sequences. Cells were defined as descendants when separation of their precursor was apparent on transmitted-light images. BisQuit has been designed for optimized detection of elongated objects, such as rod-shaped bacteria. The algorithm proceeds through successive steps of image preprocessing, object ridge tracing, tracking and segmentation. Tracing and tracking steps are interactive, permitting editing that automatically propagates to subsequent images in the sequence. This allows computation of total image intensity, mean intensity and pole-to-pole length of individual cells (Mariani, 2013).

Mouse Infections

C57BL/6 8 week-old female mice (Jackson Labs) were infected with about 100 CFU of Mtb H37Rv by using an Inhalation Exposure System (Glas-Col). Mid-log phase Mtb was washed once in PBS + 0.02% tyloxapol and centrifuged at 120 *g* to remove clumps. The inoculum (6 ml, adjusted to an OD_{580} = 0.3) was nebulized for 40 min. At indicated time points, mice were euthanatized and the lungs (right lobe and left middle and lower lobes) and spleen were homogenized in PBS and plated with and without serial dilution on 7H10-OADC agar at 37°C for 3 weeks for determination of colony-forming units (CFU). The upper lobe of the left lung was fixed in 10% formalin in PBS and sectioned for histology.

MICs

Strains were grown in 7H9 to mid-log phase, diluted to an OD of 0.06 and dispensed in 100 μL to each well of 96-well plates containing 100 μL of serial dilutions of the drug. Plates were incubated at 37 °C and OD_{580nm} was recorded at days 7, 10, 13, 15, 17, and

20. The lowest concentration of drug that reduced the OD > 90% from that in the DMSO control was called the MIC_{90}.

References

de Chaumont, F., Dallongeville, S., Chenouard, N., Hervé, N., Pop, S., Provoost, T., Meas-Yedid, V., Pankajakshan, P., Lecomte, T., Le Montagner, Y.*, et al.* (2012). Icy: an open bioimage informatics platform for extended reproducible research. Nat Methods *9*, 690-696.

Dukan, S., Farewell, A., Ballesteros, M., Taddei, F., Radman, M., and Nyström, T. (2000). Protein oxidation in response to increased transcriptional or translational errors. Proc Natl Acad Sci U S A *97*, 5746-5749.

Dukan, S., and Nyström, T. (1999). Oxidative stress defense and deterioration of growth-arrested *Escherichia coli* cells. J Biol Chem *274*, 26027-26032.

Gurskaya, N.G., Verkhusha, V.V., Shcheglov, A.S., Staroverov, D.B., Chepurnykh, T.V., Fradkov, A.F., Lukyanov, S., and Lukyanov, K.A. (2006). Engineering of a monomeric green-to-red photoactivatable fluorescent protein induced by blue light. Nat Biotechnol *24*, 461-465.

Landgraf, D., Okumus, B., Chien, P., Baker, T.A., and Paulsson, J. (2012). Segregation of molecules at cell division reveals native protein localization. Nat Methods *9*, 480-482.

Maisonneuve, E., Ducret, A., Khoueiry, P., Lignon, S., Longhi, S., Talla, E., and Dukan, S. (2009). Rules governing selective protein carbonylation. PLoS One *4*, e7269.

Mariani, O. (2013). Cell tracking in live cell imaging.

Meijler, M.M., Kaufmann, G.F., Qi, L., Mee, J.M., Coyle, A.R., Moss, J.A., Wirsching, P., Matsushita, M., and Janda, K.D. (2005). Fluorescent cocaine probes: a tool for the selection and engineering of therapeutic antibodies. J Am Chem Soc *127*, 2477-2484.

Olivo-Marin, J.-C. (2002). Extraction of spots in biological images using multiscale products. Pattern Recognition *35*, 1989-1996.

Romieu, A., Brossard, D., Hamon, M., Outaabout, H., Portal, C., and Renard, P.Y. (2008). Postsynthetic derivatization of fluorophores with alpha-sulfo-beta-alanine dipeptide linker. Application to the preparation of water-soluble cyanine and rhodamine dyes. Bioconjug Chem *19*, 279-289.

Santi, I., Dhar, N., Bousbaine, D., Wakamoto, Y., and McKinney, J.D. (2013). Single-cell dynamics of the chromosome replication and cell division cycles in mycobacteria. Nat Commun *4*, 2470.

Tamarit, J., Cabiscol, E., and Ros, J. (1998). Identification of the major oxidatively damaged proteins in *Escherichia coli* cells exposed to oxidative stress. J Biol Chem *273*, 3027-3032.

Unser, M., and Chenouard, N. (2013). A Unifying Parametric Framework for 2D Steerable Wavelet Transforms. SIAM Journal on Imaging Sciences *6*, 102-135.

van Kessel, J.C., and Hatfull, G.F. (2007). Recombineering in Mycobacterium tuberculosis. Nat Methods *4*, 147-152.

Wakamoto, Y., Dhar, N., Chait, R., Schneider, K., Signorino-Gelo, F., Leibler, S., and McKinney, J.D. (2013). Dynamic persistence of antibiotic-stressed mycobacteria. Science *339*, 91-95.